NACA RM E55G21a

NACA

RESEARCH MEMORANDUM

PERFORMANCE CHARACTERISTICS OF SEVERAL

DIVERGENT-SHROUD AIRCRAFT EJECTORS

By William K. Greathouse and William T. Beale

Lewis Flight Propulsion Laboratory
Cleveland, Ohio

CLASSIFICATION CHANGED

To UNCLASSIFIED   2

By authority of *NASA Ltr* Date *Dec. 18, 1962* *By HHR.*
dtd Nov. 14, 1962, s/Boyd Myers II. *effective date: July 17, 1962.*

NATIONAL ADVISORY COMMITTEE
FOR AERONAUTICS
WASHINGTON
September 8, 1955

3772

T-1 ,

NATIONAL ADVISORY COMMITTEE FOR AERONAUTICS

RESEARCH MEMORANDUM

PERFORMANCE CHARACTERISTICS OF SEVERAL

DIVERGENT-SHROUD AIRCRAFT EJECTORS

By William K. Greathouse and William T. Beale

SUMMARY

Ten divergent- and two cylindrical-shroud ejectors were investigated to determine internal ejector performance over a range of pressure ratios and expansion area ratios representative of flight Mach numbers up to about 3. Cold dry air was used for both the primary and secondary flows.

Experimental data and computed net-thrust characteristics indicate that variable shroud geometry is necessary for an ejector to attain near-optimum thrust performance over a typical range of flight conditions of current interest. An ejector installation having a fixed primary nozzle could maintain near-optimum net thrust if the shroud were variable from a cylindrical shape at low subsonic Mach numbers to a divergent shape at supersonic Mach numbers. A practical ejector for an afterburning turbojet is perhaps the conventional double-iris design modified so that the shroud could be either conical, cylindrical, or divergent.

INTRODUCTION

The ejector has shown merit as an aircraft jet-exit configuration because of its ability to expand the engine gases efficiently and to provide cooling from the flow of secondary air. As part of an over-all program to study various jet exits, several types of model and full-size ejectors have been investigated at the NACA Lewis laboratory. Published reports present performance data for conical ejectors (refs. 1 to 7), cylindrical ejectors (refs. 8 to 11), double-shroud ejectors (refs. 12 to 15), and divergent ejectors of low divergence angles (ref. 16). In addition, various ejector configurations have been investigated with external flow (refs. 17 to 21).

A desirable jet exit, of course, is one that can maintain high thrust performance over a wide range of operation. Such could be realized if the high thrust of the convergent-divergent nozzle at design pressure ratios could be combined with ejector thrust characteristics at below-design pressure ratios. Thus, it is reasoned that divergent-shroud ejectors might have good thrust performance over a certain desired range of operation. Analysis of divergent-ejector data in reference 16 indicates slightly better thrust for divergent shrouds than for cylindrical shrouds, even though the divergence angles were only about 3°. However, the data were limited to only four divergent ejectors, representing expansion ratios for flight Mach numbers up to about 1.3. Therefore, the purpose of this investigation is to determine and study the internal performance of ejectors with divergence angles up to about 12° and expansion ratios for flight Mach numbers up to about 3.

Ten divergent-shroud ejectors were investigated, and two cylindrical ejectors are included for comparison. Exit diameter ratios of about 1.23, 1.45, and 1.82 were selected for the divergent ejectors to represent design Mach numbers of about 1.5, 2.0, and 2.8, respectively. For each exit diameter ratio, the shroud divergence angle and annular secondary-flow area were varied, while shroud length (spacing ratio) was constant. A divergent ejector of 1.70 exit diameter ratio is also included to simulate a geometry that may be encountered with a fixed-shroud ejector when the primary nozzle of a turbojet is positioned for nonafterburning operation. Exit diameter ratios of the two cylindrical ejectors were 1.10 and 1.46. For most configurations, primary pressure ratio ranged from 1.5 to above 20, and the weight-flow ratio ranged from 0 to about 0.20. Dry air (-20° F dewpoint) at about 540° R (80° F) was used for both primary and secondary flows.

Jet-thrust and air-handling performance data are presented for each configuration. Net thrust of certain configurations is shown at typical operating conditions to indicate the internal performance of fixed and variable ejector geometry at design and off-design Mach numbers.

APPARATUS AND INSTRUMENTATION

Ejector Configurations

The geometries of the ten divergent and two cylindrical ejectors used in the investigation are listed in table I. The three groups of divergent ejectors having exit diameter ratios D_e/D_p of about 1.23, 1.45, and 1.82 represent typical expansion ratios for design Mach numbers of about 1.5, 2.0, and 2.8, respectively. Shroud divergence angle β, approach angle α, and secondary diameter D_s were varied within each group. Shroud length L was increased with exit diameter ratio

3772

CI-1 back

to keep the divergence angle under 12° and thereby avoid rapid expansion within the ejector shroud. The ejector with 1.70 exit diameter ratio represents a geometry that could occur in a fixed-shroud divergent ejector designed for afterburning but operating at nonafterburning conditions (closed primary nozzle). Two cylindrical ejectors (D_e/D_p of 1.10 and 1.46) are included for comparison with divergent-ejector performance.

Test Facility

The ejectors were installed in the test chamber photographed in figure 1(a) and shown schematically in figure 1(b). The ejector and air-supply lines were freely suspended in the chamber by four flexure rods. The resultant axial force acting on the ejector installation was transmitted through a flexure-plate-supported bell crank and linkage to a null-type force-measuring cell. Any pressure gradient on the diffuser portion of the primary-air line was prevented by a vent between the labyrinth seals that kept air flow through the second seal at a minimum. Details of this nozzle test facility are presented in reference 22.

Instrumentation

Pressures and temperatures were measured at the various stations indicated in figures 1(b) and 2. The type of measurement at each location is given in table II. Ambient exhaust pressure was measured in several places near the outside of the ejector exit.

PROCEDURE

The performance of each ejector was obtained over a range of primary pressure ratios P_p/p_0 at various constant values of corrected weight-flow ratio $(w_s/w_p)\sqrt{T_s/T_p}$. For most configurations the range of P_p/p_0 was from 1.5 to above 20, with $(w_s/w_p)\sqrt{T_s/T_p}$ from 0 to about 0.20.

Preliminary tests indicated no essential difference between average total pressure measured at station p and station 3. Also, there was no difference between plenum-chamber pressure and total pressure at station s. Therefore, primary total pressure P_p and secondary total pressure P_s were evaluated for subsequent tests from measurements at station 3 and the plenum chamber, respectively.

Ejector thrust ratio F_{ej}/F_{ip} is defined herein as the ratio of
the actual ejector jet thrust to the thrust available from the primary
stream if primary mass flow were ideally expanded to exhaust pressure.
Actual ejector jet thrust F_{ej} was obtained from the measured force
after accounting for inlet momentum forces, bellmouth forces, and
labyrinth-seal forces. The ideally expanded primary thrust F_{ip} was
computed as the product of measured primary mass flow and isentropic
velocity at the existing primary pressure ratio and temperature. The
accuracy in obtaining thrust ratio F_{ej}/F_{ip} was about ±1.5 percent.

Details of the conventional computation method used for reduction
of the test data are given in reference 22. Symbols and nomenclature
used herein are defined in appendix A.

RESULTS AND DISCUSSION

Jet-Thrust and Air-Handling Characteristics

Jet-thrust and air-handling characteristics for the ten divergent
ejectors investigated and for the two cylindrical ejectors are presented
in figures 3 and 4, respectively. A calibration of the primary nozzle
in figure 5 indicates the consistent thrust and weight-flow measurements
obtained during the investigation.

Jet thrust. - Thrust characteristics in figure 3(a) are typical of
all the ejectors investigated. Each jet-thrust curve peaked at a cer-
tain value of P_p/p_0, which indicates that the flow was fully expanded.
These peaks occurred at lower values of P_p/p_0 for the higher weight-
flow ratios simply because less flow area was available for expansion
of the primary stream. Consequently, the design pressure ratio (P_p/p_0
for peak thrust) of an ejector depends upon both the physical size of
the shroud and the amount of secondary flow.

Air-handling. - Typical air-handling characteristics of the ejec-
tors investigated are also shown in figure 3(a). For any given weight-
flow ratio, the ejector total-pressure ratio became a function of only
the upstream flow conditions (stations p and s) over a wide range of
primary pressure ratios. This is characteristic of aircraft ejectors
and can result with a stable supersonic primary flow and a "choked"
secondary flow before or at the ejector shroud exit (ref. 8). A di-
vergent ejector operates in a similar manner; but, when the secondary
passage is small enough, the flow can choke at the shroud entrance
(station s) rather than farther downstream as for a cylindrical or
conical ejector.

3772

Such a choked-shroud entrance existed for most of the divergent
ejectors investigated, and the approximate weight-flow ratio at which
choking occurred is noted for each configuration on the graphs of air-
handling performance. Also, a method of computing the air-handling per-
formance of a choked-shroud ejector is described in appendix B, and com-
puted and experimental results are compared. Thus, for a divergent
ejector, it appears that the secondary flow can be limited to a desired
value by sizing the annular passage at the shroud entrance.

Net-Thrust Performance

Net-thrust performance of an ejector system should include the in-
herent drag imposed by taking secondary air aboard the aircraft.
Secondary-air drag could be full free-stream momentum or some fraction
thereof, depending on the source of air. Only a fraction of free-stream
momentum would be chargeable to the ejector system if energy of the sec-
ondary air were partly expended for some other purpose. However, subse-
quent net-thrust evaluations charge the ejector with full inlet momentum
drag, which tends to make the results conservative. Other factors be-
yond the scope of this report are the effects of external flow, inlet-
scoop drag, and drag due to fuselage or nacelle shape near the ejector
exit.

Assumed operating conditions. - Net-thrust performance was based on
the operating schedule shown in figure 6. The curve of primary pressure
ratio P_p/p_0 typically represents accelerating climb to 35,000 feet and
0.8 Mach number and then operation above 35,000 feet at Mach numbers
from 0.8 to 3.0. The curve of $(P_s/P_p)_{max}$ represents an upper limit of
ejector operation (maximum ejector total-pressure ratio) with assumed
pressure losses through the secondary system. Secondary air was consid-
ered to enter at free-stream total temperature and to experience a tem-
perature rise before reaching the ejector. Complete details of the
method used in evaluating net-thrust ratio are given in appendix C.

Performance at design Mach number. - Net-thrust performance of the
various ejectors at design Mach numbers of 1.5, 2.0, and 2.8 is shown in
figure 7 for afterburning conditions $(T_p = 3500^\circ R)$. Each curve repre-
sents operation over a range of secondary flows and total-pressure ra-
tios from $w_s/w_p = 0$ to $(P_s/P_p)_{max}$ at the respective design Mach num-
ber. As shown by the sketches and curves in figure 7, the highest net-
thrust ratio at each design Mach number was attained by the divergent
ejector having the largest divergence angle and the smallest secondary-
flow passage (configurations 3, 5, and 10). In other words, a higher
net thrust occurred as the ejector geometry approached that of a simple
convergent-divergent nozzle.

At maximum total-pressure ratio $(P_s/P_p)_{max}$, ejectors 3, 5, and 10 could handle small secondary flows $\left((w_s/w_p)\sqrt{T_s/T_p}\right.$ from 0.02 to about 0.04$\left.\right)$ and maintain a net thrust of only about 1 percent less than that of a good uncooled convergent-divergent nozzle (velocity coefficient of 0.98). Cooling a convergent-divergent nozzle would certainly produce a net-thrust decrease (about 1-percent thrust decrease for each percent of compressor air used). Thus, it appears that, for a fixed jet-exit configuration at design Mach number, a divergent-shroud ejector design could produce a net thrust equal to or slightly higher than a cooled convergent-divergent nozzle. However, if for some reason cooling of a convergent-divergent nozzle were unnecessary, the convergent-divergent nozzle would of course be superior to the ejector charged with full free-stream inlet momentum of the secondary air.

The net-thrust performance of the Mach 2.0 design cylindrical ejector is lower than for any of the divergent ejectors (fig. 7(b)), because the cylindrical ejector requires greater secondary flows (and hence a larger inlet momentum drag) for efficient expansion of the primary stream. The peak shown in the cylindrical-ejector thrust curve indicates that, for corrected weight-flow ratios above 0.04, the inlet momentum drag exceeded any jet-thrust increase produced by flowing additional secondary air.

Performance over range of Mach numbers. - Net-thrust performance of the three divergent ejectors that previously showed the best net thrust at design Mach numbers of 1.5, 2.0, and 2.8 (configurations 3, 5, and 10, respectively) is presented in figure 8(a) over a range of flight conditions up to design Mach number. For each configuration, peak net thrust occurred very near the design Mach number, and large overexpansion losses are indicated at below-design Mach number. Thus, the high net-thrust characteristics of a fixed-shroud divergent ejector are realized only for operation near design conditions. This undesirable characteristic could not be relieved by control of secondary air but could be eliminated by use of variable shroud geometry.

Net-thrust performance of the two cylindrical ejectors investigated is shown in figure 8(b) over a range of Mach number. Ejector 11 shows good net-thrust characteristics up to Mach number of about 1.0, above which underexpansion losses became excessive as in the case of a simple conical nozzle. Ejector 12 shows higher net thrust than a comparable divergent ejector (configuration 5, fig. 8(a)) up to Mach number of about 1.2. Above Mach 1.3 the secondary air handled by the cylindrical ejector increased rapidly and thus produced a sharp net-thrust decrease due to excessive inlet momentum drag. By progressively throttling the secondary flow to a corrected weight flow of about 0.04 at Mach 2.0, the net thrust could be maintained at about 91 percent, as shown by the

3772

dashed curve in figure 8(b). Throttling the flow below 0.04 would de-
crease the net thrust at Mach 2.0 below 91 percent, until at zero sec-
ondary flow the net thrust would be about 86 percent.

It has long been realized that fixed-shroud ejector characteristics
are in direct contrast to those desired when primary-nozzle area is mod-
ulated for an afterburning turbojet engine. To further illustrate this
point for the case of a fixed-shroud divergent ejector, the net-thrust
performance of such an installation is represented in figure 9. The
comparison is between a divergent ejector (configuration 5) representing
a design for afterburning (3500° R) at Mach 2.0 with a corrected weight-
flow ratio of about 0.04, and the ejector resulting from closing the
primary nozzle (configuration 7) for nonafterburning operation (1600° R).
The very low net thrust at nonafterburning is the combined result of
overexpansion and excessive secondary inlet momentum drag. Throttling
the secondary flow in this case would reduce the net thrust even more,
because the overexpansion losses would increase more than the inlet mo-
mentum drag would decrease.

Variable ejector geometry. - From previous curves of fixed-ejector
performance, it is apparent that variable geometry is required for an
ejector to maintain near-optimum net thrust over the range of operating
conditions of current interest.

An ejector installation using a fixed primary nozzle could attain
near-optimum thrust if the shroud could be varied from cylindrical at
low Mach number to divergent at high Mach number. The performance of
such an ejector is illustrated in figures 10(a) and (b) for afterburning
(3500° R) and nonafterburning (1600° R), respectively. The curves are
the locus of net thrust at design pressure ratio for several fixed ejec-
tors investigated and thus represent maximum ejector thrust performance
over the assumed flight schedule. The over-all shroud variation indi-
cated (fig. 10(a)) for the typical schedule used herein would be from a
cylindrical ejector with 1.10 diameter ratio at low subsonic Mach num-
bers to a divergent ejector with 1.82 exit diameter ratio at Mach 2.8.
For a different flight schedule, the over-all shroud variation will, of
course, depend on the schedule itself and on the upper Mach number
limit, since the divergent shroud must provide the proper expansion ra-
tio for the combined flows. At the largest expansion ratio (largest
shroud exit), the shroud divergence angle should be small enough to pre-
vent rapid expansion of the flow. Divergence angles for the ejectors
investigated were less than 12°, but a shorter ejector resulting from
angles up to 15° or 20° might represent a reasonable design compromise
with respect to weight and size.

To attain near-optimum net thrust for a turbojet-afterburner ejec-
tor installation, both a variable shroud-inlet diameter ratio D_s/D_p

and a variable exit diameter ratio D_e/D_p would be necessary. However, such a configuration might be impractical because of complex mechanical design. A more practical design would be the conventional double-iris conical ejector modified so that the shroud could further expand to form cylindrical and divergent shrouds when the afterburner is in operation. General trends that can be expected for this type of installation are illustrated by the curves and sketches in figure 10(c). The curve abc is for conical-ejector shroud variation between an exit diameter ratio of about 1.10 and 1.30 with the afterburner off (1600° R). The curve defg is for shroud variation from an exit diameter ratio of 1.10 (cylindrical) to 1.82 (divergent) with the afterburner on (3500° R). Net-thrust ratio is lower for nonafterburning than for afterburning because inlet momentum of both the primary and the secondary system is a greater proportion of the available jet thrust at 1600° than at 3500° R. In general, the ejector net thrust is indicated as about 1 percent less than optimum nozzle net thrust for afterburning conditions and about 2 percent less for nonafterburning conditions.

CONCLUDING REMARKS

Ten divergent- and two cylindrical-shroud ejectors were investigated. The results indicate that variable shroud geometry is necessary for an ejector to maintain near-optimum thrust performance over a typical range of flight conditions of current interest.

The afterburning turbojet and ejector installation requires both a variable shroud exit and a variable shroud entrance (which involves complex mechanical design) in order to maintain optimum thrust characteristics as the primary nozzle is varied. A more practical ejector for an afterburning turbojet is perhaps the conventional double-iris design modified so that the shroud could be either conical, cylindrical, or divergent.

An ejector installation having a fixed primary nozzle could attain near-optimum thrust over a range of flight Mach numbers if the shroud geometry were variable from cylindrical to divergent. A cylindrical shroud of about 1.10 diameter ratio would serve for low subsonic Mach numbers. At supersonic Mach numbers, a divergent shroud providing the necessary expansion ratio with divergence angles up to 15° or 20° would have adequate performance.

Use of an ejector for a fixed jet-exit application depends somewhat on cooling-air requirements. For no cooling air, a fixed convergent-divergent type nozzle could provide about 1 percent more thrust than an ejector. With corrected cooling-air-flow ratios of about 0.02 to 0.04, the divergent ejector apparently can provide a net thrust equal to or slightly better than the net thrust expected from a cooled convergent-divergent nozzle.

For most of the divergent ejectors investigated, secondary flow was choked in the annular passage at the ejector entrance for high values of weight-flow ratio. Air-handling characteristics for such choked operation can be computed from one-dimensional flow theory within an accuracy of about 0.01 weight-flow-ratio unit.

Lewis Flight Propulsion Laboratory
    National Advisory Committee for Aeronautics
        Cleveland, Ohio, July 27, 1955

APPENDIX A

SYMBOLS

A	area, sq ft
C	coefficient
D	diameter, in. or ft
F	thrust, lb
g	acceleration due to gravity, 32.17 ft/sec^2
L	distance between exits of primary nozzle and ejector shroud, in. or ft
M	Mach number
P	total pressure, lb/sq ft
p	static pressure, lb/sq ft
R	gas constant, 53.3 ft-lb/(lb)($^{\circ}$R)
T	total temperature, $^{\circ}$R
t	static temperature, $^{\circ}$R
V	velocity, ft/sec
w	weight flow, lb/sec
α	half cone angle of upstream shroud section, deg
β	wall divergence angle of ejector shroud, deg
γ	ratio of specific heats
δ	ratio of local pressure to NACA standard sea-level pressure of 2116 lb/sq ft
θ	ratio of local temperature to NACA standard sea-level temperature of 518.7° R
ρ	density, lb/cu ft

3772

Subscripts:

b	bellmouth
c	cold
e	ejector exit
ej	ejector
F	thrust
h	hot
ip	isentropic primary expansion
j	jet
n	net
p	primary stream or station p
s	secondary stream or station s
v	velocity
O	free stream or ambient exhaust

Parameters:

$\dfrac{A_s}{A_p}$ secondary area ratio (annular passage) $= \left(\dfrac{D_s}{D_p}\right)^2 - 1$

C_F thrust coefficient, $\dfrac{\text{actual jet thrust}}{(\text{actual mass flow})(\text{isentropic velocity})}$

C_v velocity coefficient, $\dfrac{\text{actual exit velocity}}{\text{isentropic velocity}}$

$\dfrac{D_e}{D_p}$ exit diameter ratio

$\dfrac{D_s}{D_p}$ secondary diameter ratio

$\dfrac{F_{ej}}{F_{ip}}$ thrust ratio

$\dfrac{L}{D_p}$ spacing (length) ratio

$\dfrac{P_p}{p_0}$ primary pressure ratio

$\dfrac{P_s}{P_p}$ ejector total-pressure ratio

$\dfrac{T_p}{T_s}$ ejector temperature ratio

$\dfrac{w_s}{w_p}$ ejector weight-flow ratio

$\dfrac{w_s}{w_p}\sqrt{\dfrac{T_s}{T_p}}$ corrected weight-flow ratio

APPENDIX B

AIR-HANDLING CHARACTERISTICS OF CHOKED EJECTOR

Consider the choked ejector system in sketch (a):

$$P_s, A_s, T_s$$
$$M_s = 1.0$$
$$P_p, A_p, T_p$$
$$M_p = 1.0$$
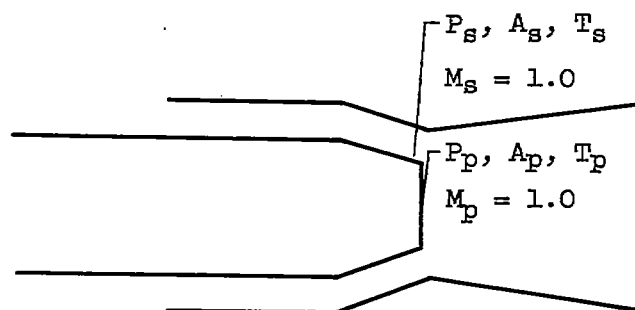
Sketch (a)

Since both primary and secondary Mach numbers are 1.0 at a known flow area, the flow through each system can be expressed for the primary stream as

$$w_p = C_p(\rho AV)_p = C_p P_p A_p \sqrt{\frac{\gamma_p g}{RT_p}} \frac{\sqrt{\frac{\gamma_p + 1}{2}}}{\left(\frac{\gamma_p + 1}{2}\right)^{\frac{\gamma_p}{\gamma_p - 1}}} \tag{B1}$$

and for the secondary stream as

$$w_s = C_s(\rho AV)_s = C_s P_s A_s \sqrt{\frac{\gamma_s g}{RT_s}} \frac{\sqrt{\frac{\gamma_s + 1}{2}}}{\left(\frac{\gamma_s + 1}{2}\right)^{\frac{\gamma_s}{\gamma_s - 1}}} \tag{B2}$$

where C is the flow coefficient of the corresponding passage. Combining the two equations, corrected weight-flow ratio is expressed as

$$\frac{w_s}{w_p}\sqrt{\frac{T_s}{T_p}} = \left(\frac{C_s}{C_p}\right)\left(\frac{P_s}{P_p}\right)\left(\frac{A_s}{A_p}\right)\sqrt{\frac{\gamma_s(\gamma_s+1)}{\gamma_p(\gamma_p+1)}} \frac{\left(\dfrac{\gamma_p+1}{2}\right)^{\frac{\gamma_p}{\gamma_p-1}}}{\left(\dfrac{\gamma_s+1}{2}\right)^{\frac{\gamma_s}{\gamma_s-1}}} \tag{B3}$$

Thus, the pumping characteristics of such an ejector are defined if flow areas, flow coefficients, and specific-heat ratios are known.

Computed and experimental weight-flow ratios are compared in figure 11 for several choked divergent ejectors. Agreement is generally within 0.01 w_s/w_p unit.

APPENDIX C

CALCULATION OF NET-THRUST RATIO FOR EJECTOR

Net-thrust ratio $\left(F_{ej}/F_{ip}\right)_n$ is defined herein as the ratio of the net thrust of the ejector system to the net thrust available from the primary system if the actual mass flow were expanded isentropically to exhaust pressure. In equation form,

$$\left(\frac{F_{ej}}{F_{ip}}\right)_n = \frac{F_{ej} - \dfrac{w_p}{g} V_0 - \dfrac{w_s}{g} V_0}{F_{ip} - \dfrac{w_p}{g} V_0} \tag{C1}$$

For computation purposes, the equation was rearranged by using

$F_{ej} = \left(\dfrac{F_{ej}}{F_{ip}}\right)_j F_{ip}$ and $F_{ip} = \dfrac{w_p}{g} V_{ip}$ and dividing through by $\dfrac{w_p}{g} V_{ip}$ to

obtain

$$\left(\frac{F_{ej}}{F_{ip}}\right)_n = \frac{\left(\dfrac{F_{ej}}{F_{ip}}\right)_j - \left(\dfrac{w_s}{w_p} + 1\right) \dfrac{V_0}{V_{ip}}}{1 - \dfrac{V_0}{V_{ip}}} \tag{C2}$$

In order to evaluate the performance of a hot (hot primary stream) ejector from the cold data herein, the following two assumptions were made: (1) The corrected weight-flow ratio $(w_s/w_p)\sqrt{T_s/T_p}$ of a hot ejector is equal to the corrected weight-flow ratio of a cold ejector, and (2) the jet-thrust ratio of a hot ejector is the same as for a cold ejector at the same over-all operating pressure ratios. Thus, equation (C2) becomes

$$\left(\frac{F_{ej}}{F_{ip}}\right)_n = \frac{\left(\dfrac{F_{ej}}{F_{ip}}\right)_{j,c} - \left(\dfrac{V_0}{V_{ip}}\right)_h \left[\left(\dfrac{w_s}{w_p}\sqrt{\dfrac{T_s}{T_p}}\right)_c \left(\sqrt{\dfrac{T_p}{T_s}}\right)_h + 1\right]}{1 - \left(\dfrac{V_0}{V_{ip}}\right)_h} \tag{C3}$$

and net-thrust ratio can be evaluated for a typical schedule of flight conditions.

The net-thrust values computed herein are based on a typical schedule of primary pressure ratio and maximum ejector total-pressure ratio

with flight Mach number and altitude as shown in figure 7. The procedure for computing $(F_{ej}/F_{ip})_n$ from equation (C3) is as follows.

(1) Choose Mach number and primary temperature. Determine P_p/P_0 and $(P_s/P_p)_{max}$ from schedule.

(2) Select an ejector to be evaluated. From its cold performance data at P_p/P_0, get values of $(F_{ej}/F_{ip})_{j,c}$ and $\left(\dfrac{w_s}{w_p}\sqrt{\dfrac{T_s}{T_p}}\right)_c$ from $w_s/w_p = 0$ to $(P_s/P_p)_{max}$.

(3) Compute (V_0/V_{ip}) as follows:

$$\frac{V_0}{V_{ip}} = \frac{M_0\sqrt{(1.4)\left(\dfrac{t_0}{T_p}\right)}}{\left(\dfrac{V}{\sqrt{gRT}}\right)_{ip}} \tag{C4}$$

where t_0 is the altitude temperature in °R and $(V/\sqrt{gRT})_{ip}$ is a velocity parameter from tables of reference 23 corresponding to the P_p/P_0 at a typical γ_p of 1.3.

(4) Compute T_s as follows:

$$T_s = T_0 + (\Delta T)_s \tag{C5}$$

where T_0 is the free-stream total temperature, and $(\Delta T)_s$ is the temperature rise through the secondary system for a specific secondary flow. In this report $(\Delta T)_s$ was evaluated by the methods of reference 24.

(5) Solve equation (C3) for $(F_{ej}/F_{ip})_n$ and plot:

M_0 = constant
T_p = constant
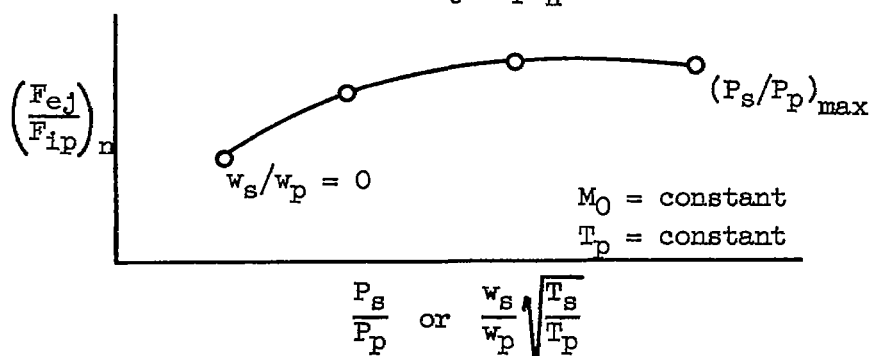
(6) Repeat (1) to (5) at other values of Mach number to obtain performance curves over the desired range of Mach number.

REFERENCES

1. Huddleston, S. C., Wilsted, H. D., and Ellis, C. W.: Performance of Several Air Ejectors with Conical Mixing Sections and Small Secondary Flow Rates. NACA RM E8D23, 1948.

2. Wilsted, H. D., Huddleston, S. C., and Ellis, C. W.: Effect of Temperature on Performance of Several Ejector Configurations. NACA RM E9E16, 1949.

3. Ellis, C. W., Hollister, D. P., and Sargent, A. F., Jr.: Preliminary Investigation of Cooling-Air Ejector Performance at Pressure Ratios from 1 to 10. NACA RM E51H21, 1951.

4. Wallner, Lewis E., and Jansen, Emmert T.: Full-Scale Investigation of Cooling Shroud and Ejector Nozzle for a Turbojet Engine - Afterburner Installation. NACA RM E51J04, 1951.

5. Greathouse, W. K., and Hollister, D. P.: Preliminary Air-Flow and Thrust Calibrations of Several Conical Cooling-Air Ejectors with a Primary to Secondary Temperature Ratio of 1.0. I - Diameter Ratios of 1.21 and 1.10. NACA RM E52E21, 1952.

6. Greathouse, W. K., and Hollister, D. P.: Preliminary Air-Flow and Thrust Calibrations of Several Conical Cooling-Air Ejectors with a Primary to Secondary Temperature Ratio of 1.0. II - Diameter Ratios of 1.06 and 1.40. NACA RM E52F26, 1952.

7. Ciepluch, C. C., and Fenn, D. B.: Experimental Data from Four Full-Scale Conical Cooling Air Ejectors. NACA RM E54F02, 1954.

8. Kochendorfer, Fred D., and Rousso, Morris D.: Performance Characteristics of Aircraft Cooling Ejectors Having Short Cylindrical Shrouds. NACA RM E51E01, 1951.

9. Greathouse, W. K., and Hollister, D. P.: Air-Flow and Thrust Characteristics of Several Cylindrical Cooling-Air Ejectors with a Primary to Secondary Temperature Ratio of 1.0. NACA RM E52L24, 1953.

10. Kochendorfer, Fred D.: Effect of Properties of Primary Fluid on Performance of Cylindrical Shroud Ejectors. NACA RM E53L24a, 1954.

11. Greathouse, W. K.: Preliminary Investigation of Pumping and Thrust Characteristics of Full-Size Cooling-Air Ejectors at Several Exhaust-Gas Temperatures. NACA RM E54A18, 1954.

12. Ellis, C. W., Hollister, D. P., and Wilsted, H. D.: Investigation of Performance of Several Double-Shroud Ejectors and Effect of Variable-Area Exhaust Nozzle on Ejector Performance. NACA RM E52D25, 1952.

13. Hollister, Donald P., and Greathouse, William K.: Performance of Double-Shroud Ejector Configuration with Primary Pressure Ratios from 1.0 to 10. NACA RM E52K17, 1953.

14. Reshotko, Eli: Performance Characteristics of a Double-Cylindrical-Shroud Ejector Nozzle. NACA RM E53H28, 1953.

15. Greathouse, William K.: Performance Characteristics of Several Full-Scale Double-Shroud Ejector Configurations over a Range of Primary Gas Temperatures. NACA RM E54F07, 1954.

16. Huntley, S. C., and Yanowitz, Herbert: Pumping and Thrust Characteristics of Several Divergent Cooling-Air Ejectors and Comparison of Performance with Conical and Cylindrical Ejectors. NACA RM E53J13, 1954.

17. Allen, John L.: Pumping Characteristics for Several Simulated Variable-Geometry Ejectors with Hot and Cold Primary Flow. NACA RM E54G15, 1954.

18. Vargo, Donald J.: Effects of Secondary-Air Flow on Annular Base Force of a Supersonic Airplane. NACA RM E54G28, 1954.

19. Hearth, Donald P., and Valerino, Alfred S.: Thrust and Pumping Characteristics of a Series of Ejector-Type Exhaust Nozzles at Subsonic and Supersonic Flight Speeds. NACA RM E54H19, 1954.

20. Salmi, Reino J.: Experimental Investigation of Drag of Afterbodies with Existing Jet at High Subsonic Mach Numbers. NACA RM E54I13, 1954.

21. Beke, Andrew, and Simon, Paul C.: Thrust and Drag Characteristics of Simulated Variable-Shroud Nozzles with Hot and Cold Primary Flows at Subsonic and Supersonic Speeds. NACA RM E54J26, 1955.

22. Krull, H. George, and Beale, William T.: Effect of Plug Design on Performance Characteristics of Convergent-Plug Exhaust Nozzles. NACA RM E54H05, 1954.

23. Turner, L. Richard, Addie, Albert N., and Zimmerman, Richard H.:
    Charts for the Analysis of One-Dimensional Steady Compressible
    Flow. NACA TN 1419, 1948.

24. Koffel, William K., and Kaufman, Harold R.: Empirical Cooling Cor-
    relation for an Experimental Afterburner with an Annular Cooling
    Passage. NACA RM E52C13, 1952.

3772

CI-3 back

TABLE I. - EJECTOR CONFIGURATIONS
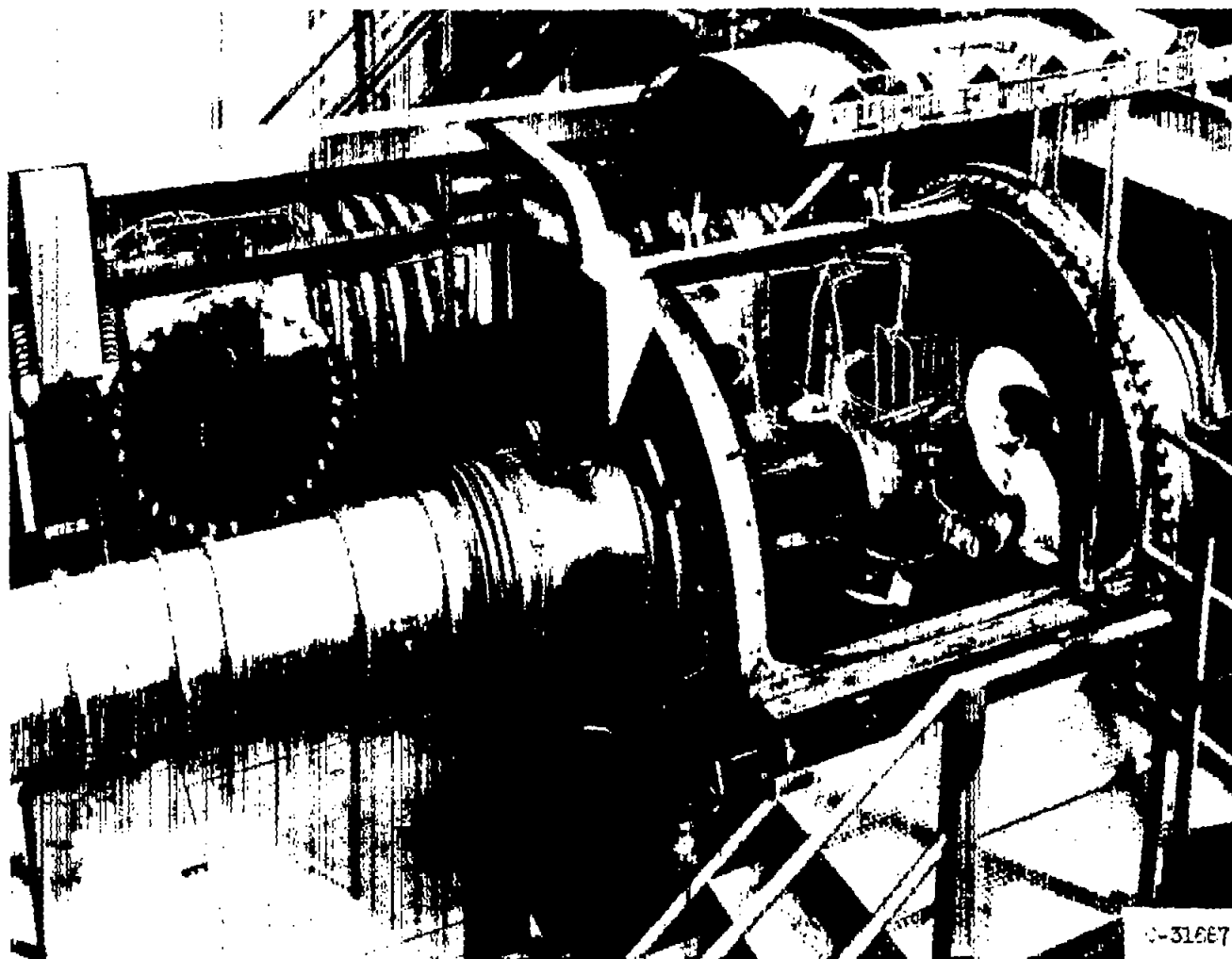

D_p = 6.018 in. inside
    = 6.143 in. outside
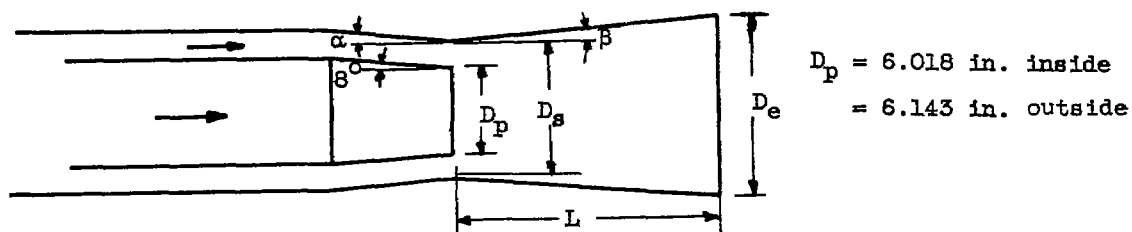
Shroud	Ejector	Exit diameter ratio, D_e/D_p	Inlet diameter ratio, D_s/D_p	Spacing ratio, L/D_p	Divergence angle, β	Approach angle, α	Data in figure
Divergent	1	1.24	1.20	0.45	2° 51'	15° 36'	3(a)
	2	1.23	1.14	.47	5° 36'	17° 34'	(b)
	3	1.23	1.04	.47	11° 31'	20° 9'	(c)
	4	1.44	1.21	1.06	6° 22'	16° 1'	(d)
	5	1.45	1.09	1.06	9° 25'	19° 7'	(e)
	6	1.46	1.09	1.07	9° 39'	90°	(f)
	7	1.70	1.34	1.07	9° 23'	11° 54'	(g)
	8	1.82	1.26	1.91	8° 20'	13° 53'	(h)
	9	1.81	1.21	1.91	8° 59'	15° 28'	(i)
	10	1.82	1.10	1.90	10° 34'	19° 4'	(j)
Cylindrical	11	1.10	1.12	0.80	0°	90°	4(a)
	12	1.46	1.46	2.12	0°	90°	(b)

3772

TABLE II. - INSTRUMENTATION

Station or location	Total temperature	Total pressure	Static pressure
1	-------------	Two 4-probe radial rakes	4 Wall taps
2	-------------	8-Probe diametrical rake	4 Wall taps
On outside of bellmouth inlet	-------------	-------------	Survey with 12 taps
3	3-Probe diametrical rake	8-Probe diametrical rake	-------------
Plenum chamber (secondary air)	-------------	-------------	8 Taps circumferential
Orifice (secondary air)	Single probe	-------------	(a)
p	-------------	8-Probe diametrical rake[b]	-------------
s	-------------	Three 3-probe rakes equally spaced[b]	-------------

[a]Upstream pressure and orifice differential pressure measured for calibrated orifice assembly.

[b]Installed during preliminary only.

(a) Photograph.

Figure 1. - Nozzle test facility.

Secondary-air orifice — To air-supply system

Primary-air flow
Station 2

Vent line

Flexible secondary-
air line

Flexure rod

Station 1

P_b

Station 3

Plemm
chamber

Primary-air line

To exhaust
system

Bellmouth
inlet

To air-supply
system

Labyrinth
seals

Ejector
shroud

Diffuser

CD-4510

Bedplate

Bell crank

Force-measuring cell
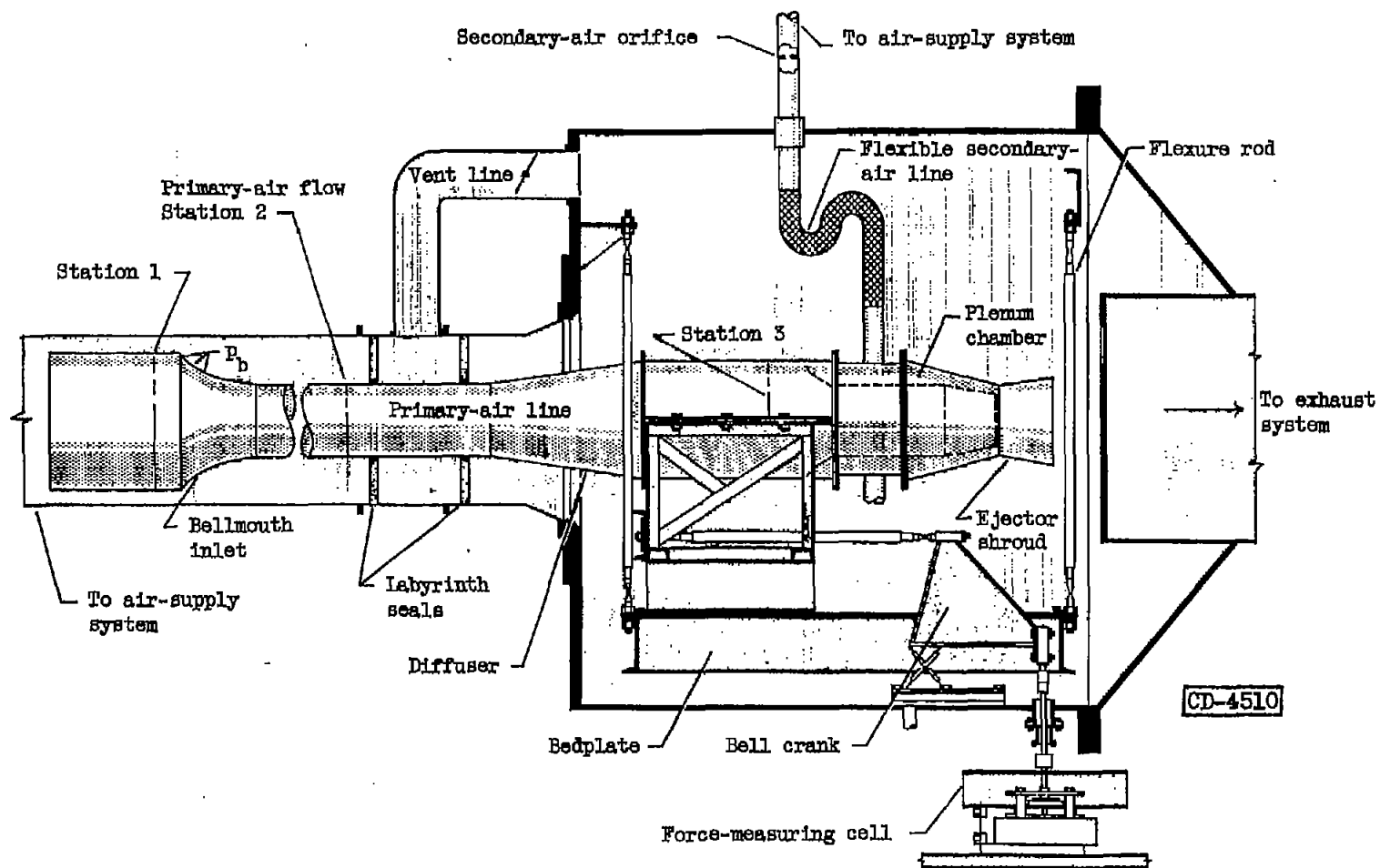
(b) Schematic diagram.

Figure 1. - Concluded. Nozzle test facility.
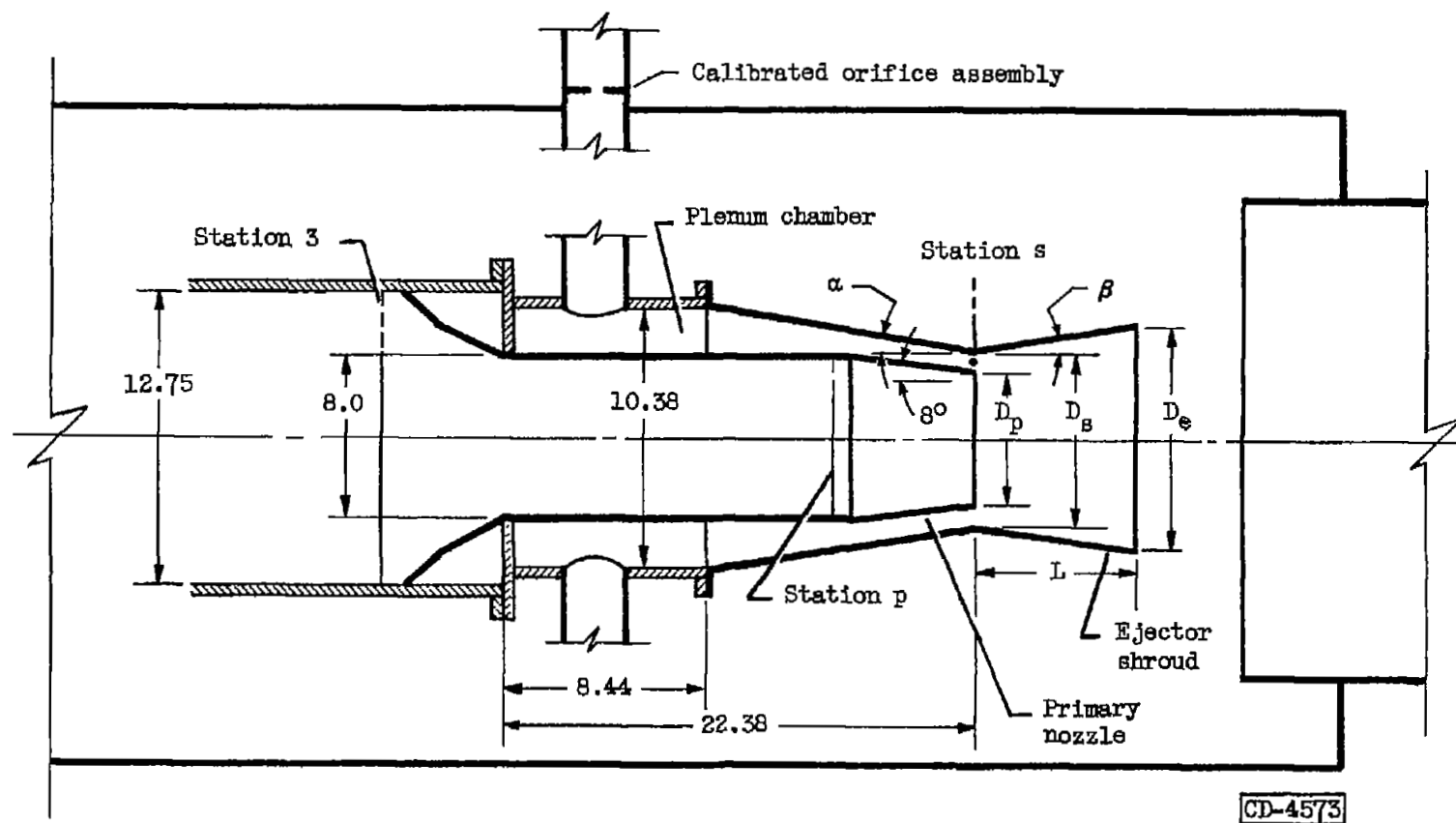
Figure 2. - Schematic diagram of typical ejector assembly. (All dimensions in inches);
D_p = 6.018 inches inside and 6.143 inches outside. (See Table 1 for other values.)

3772

CL-4
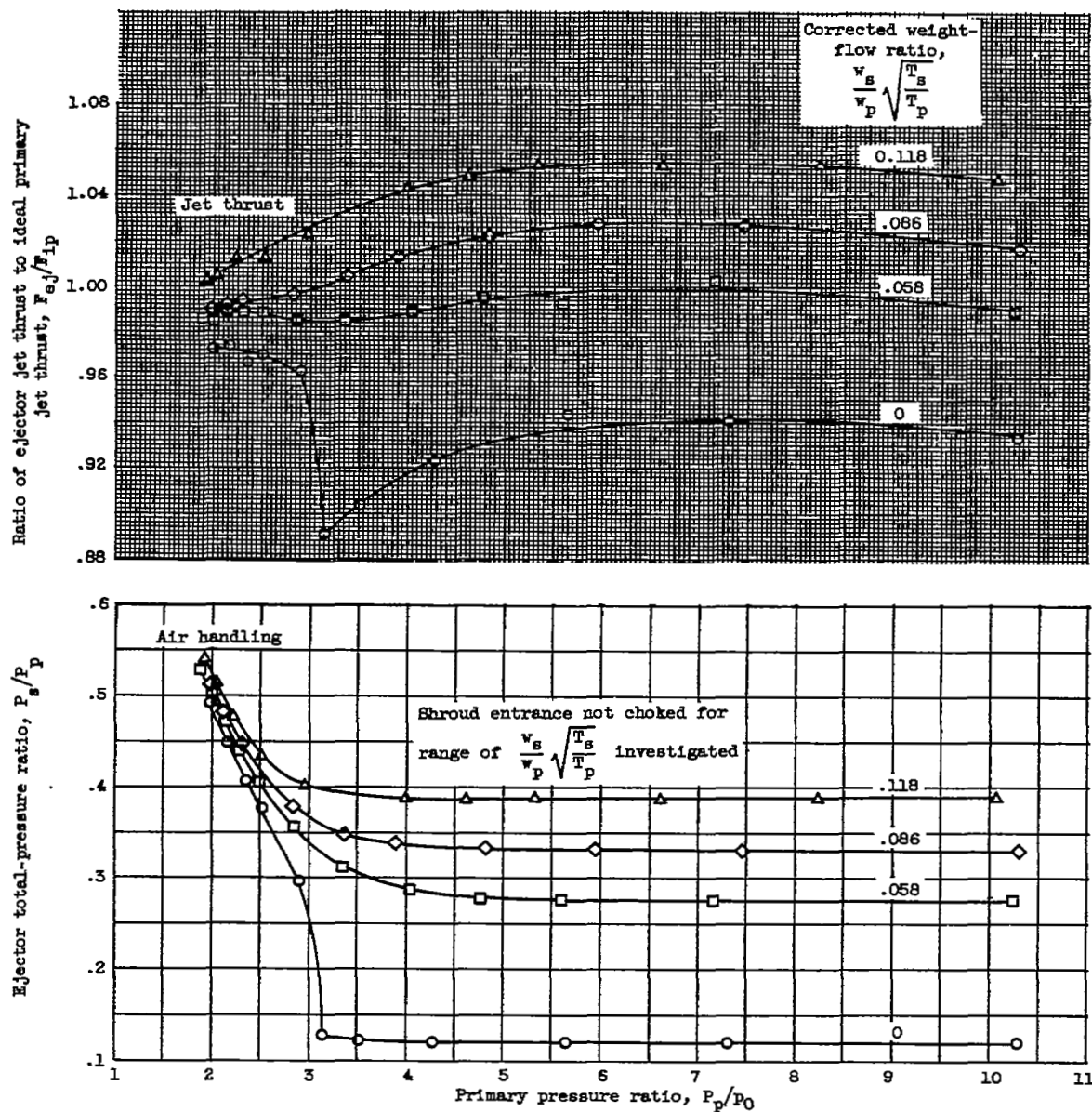
(a) Ejector 1.

Figure 3. - Performance of divergent-shroud ejectors.
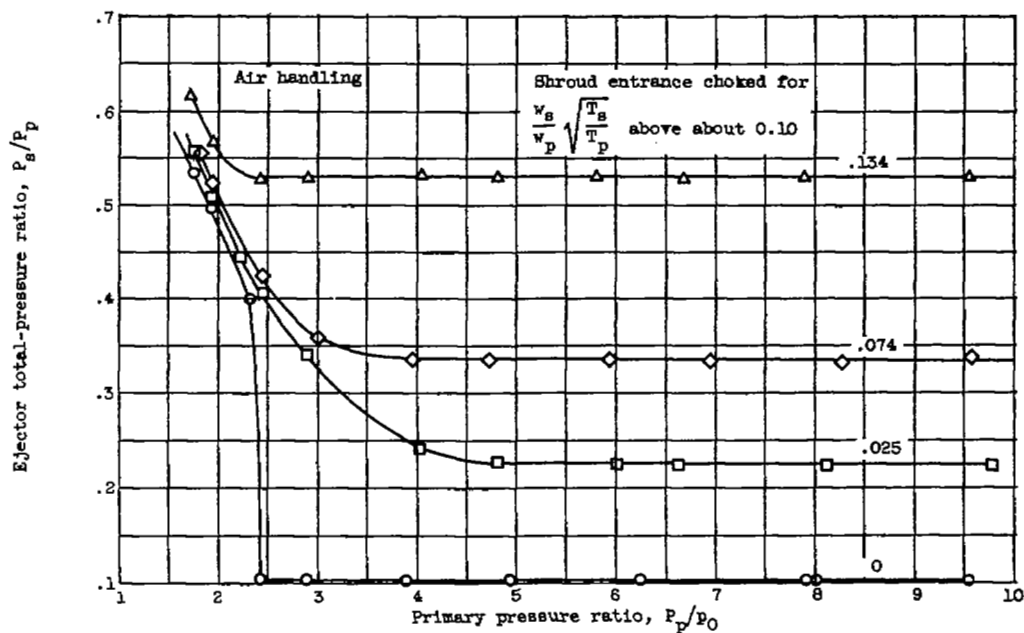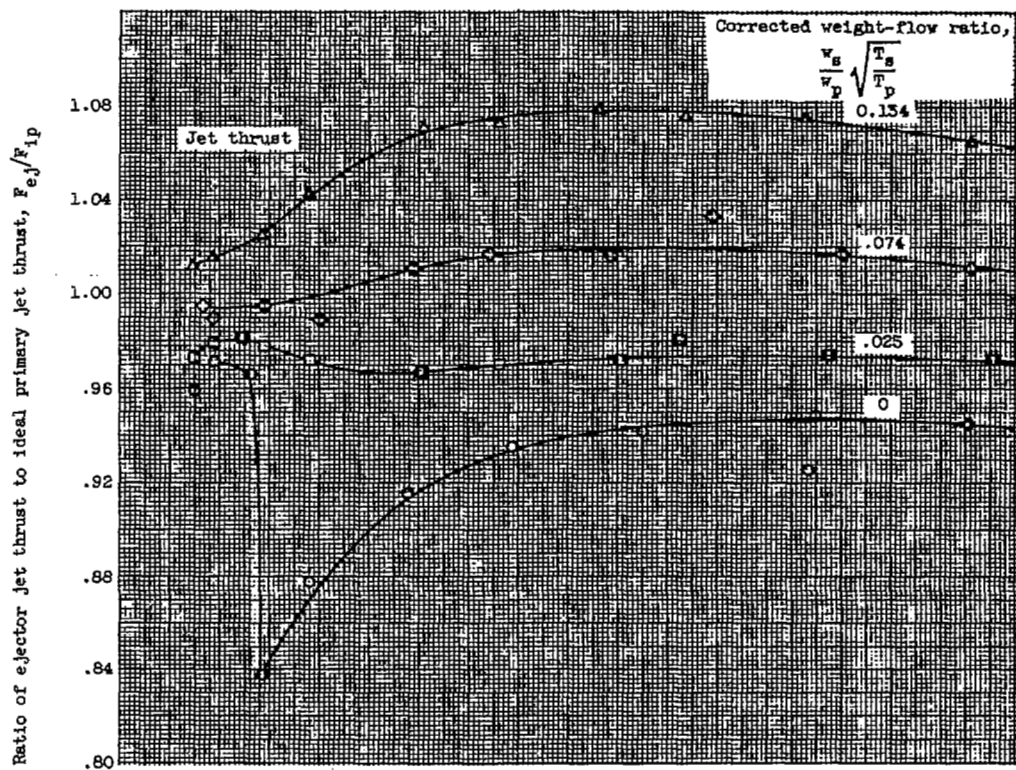
(b) Ejector 2.

Figure 3. - Continued. Performance of divergent-shroud ejectors.
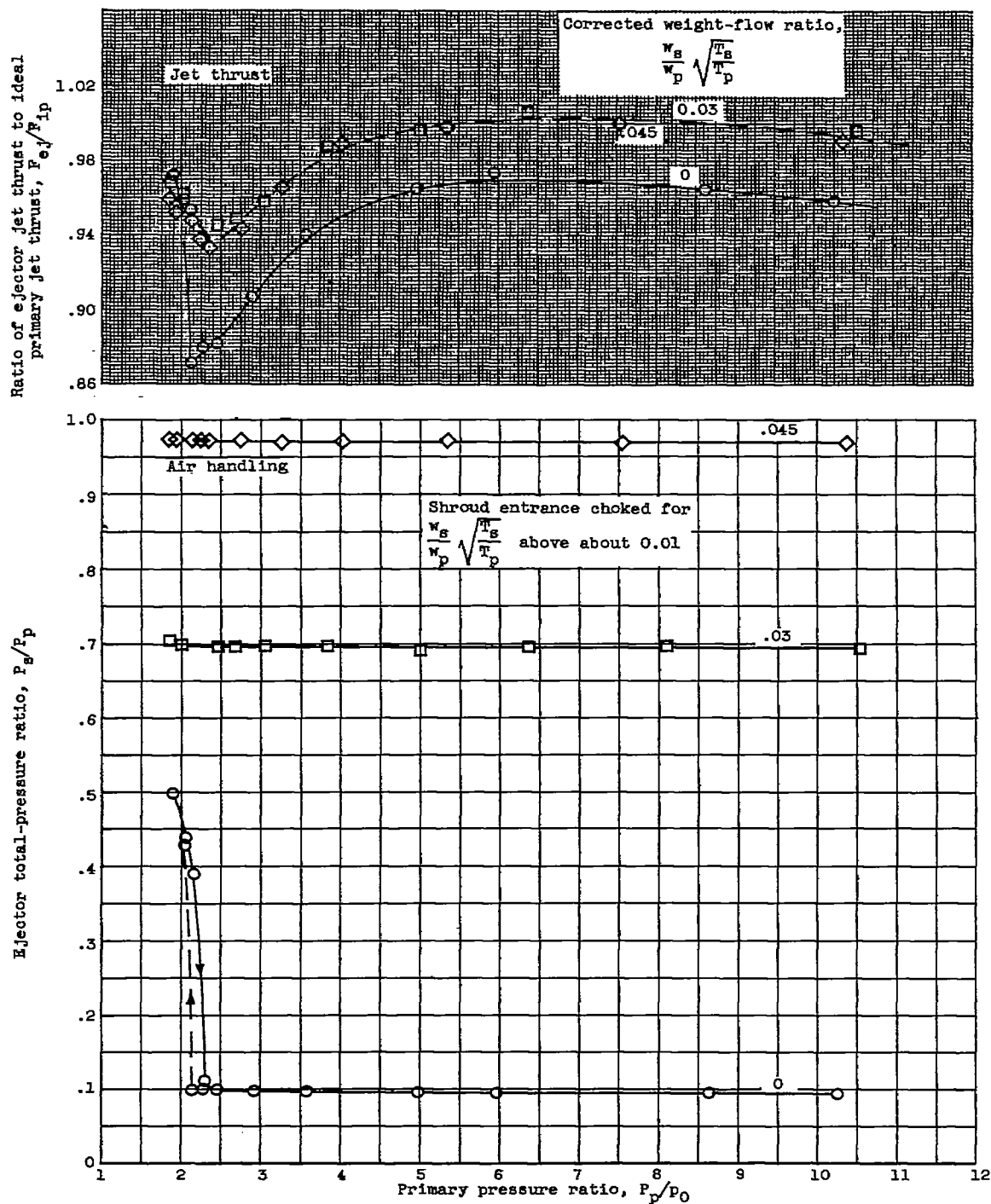
(c) Ejector 3.

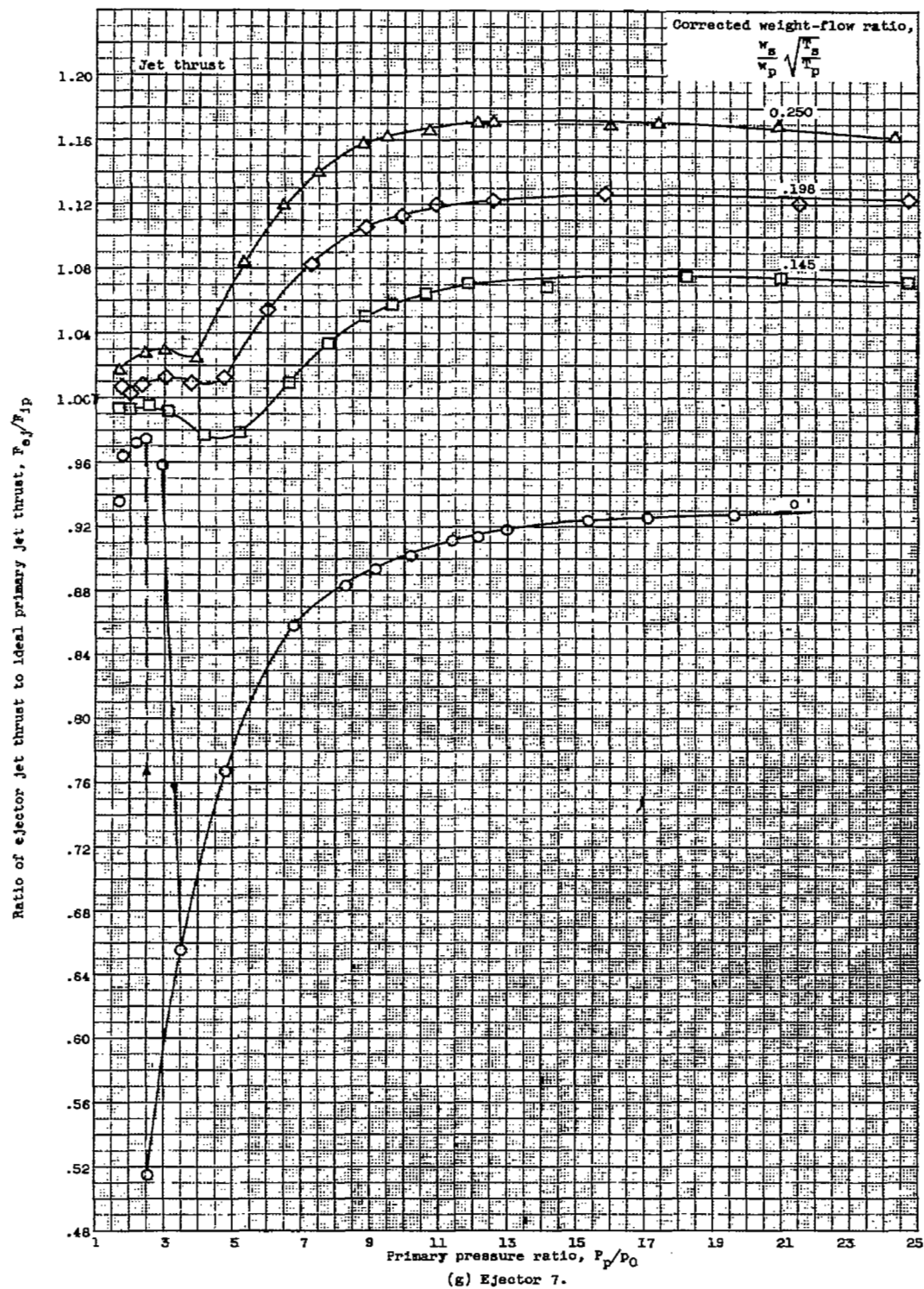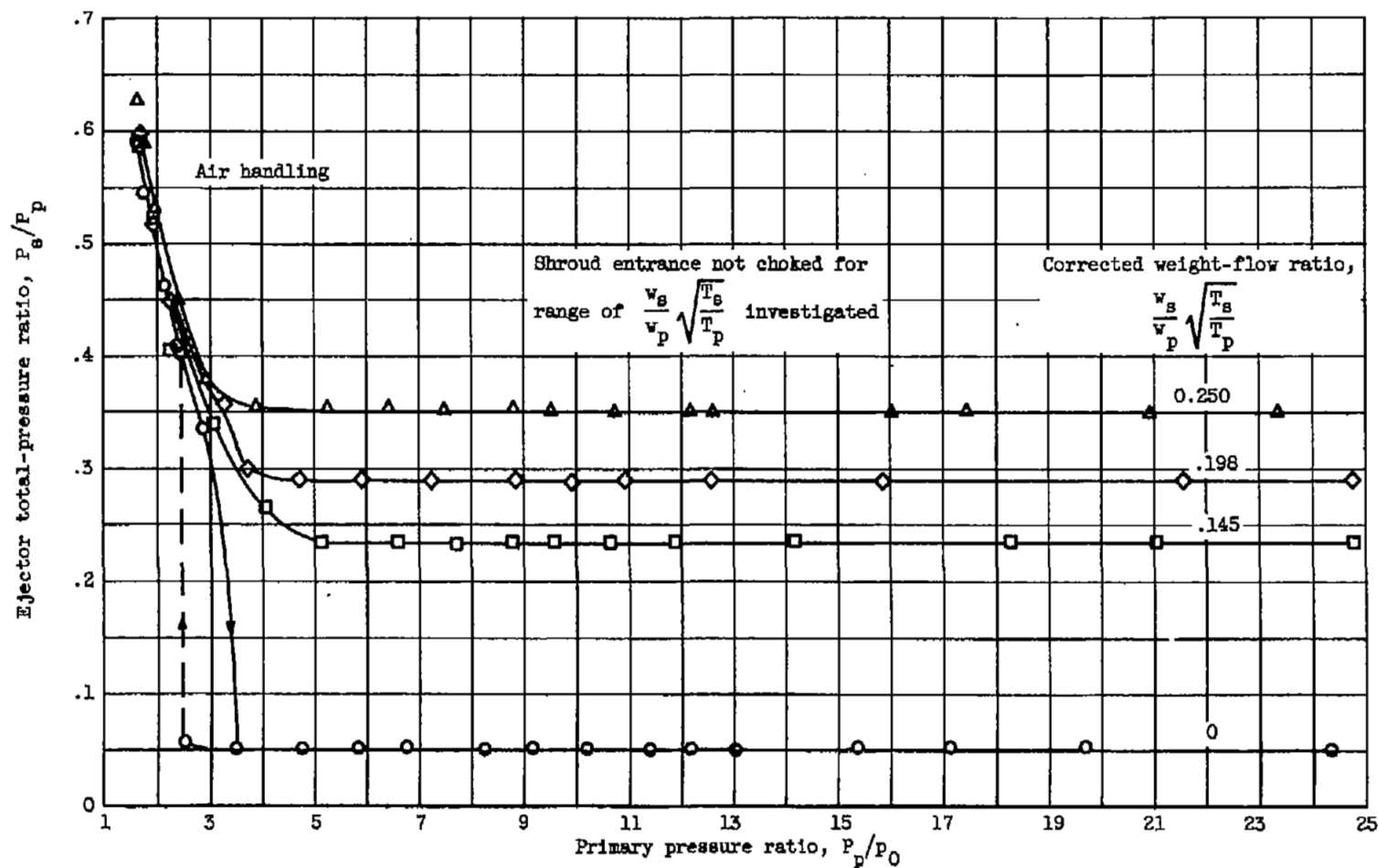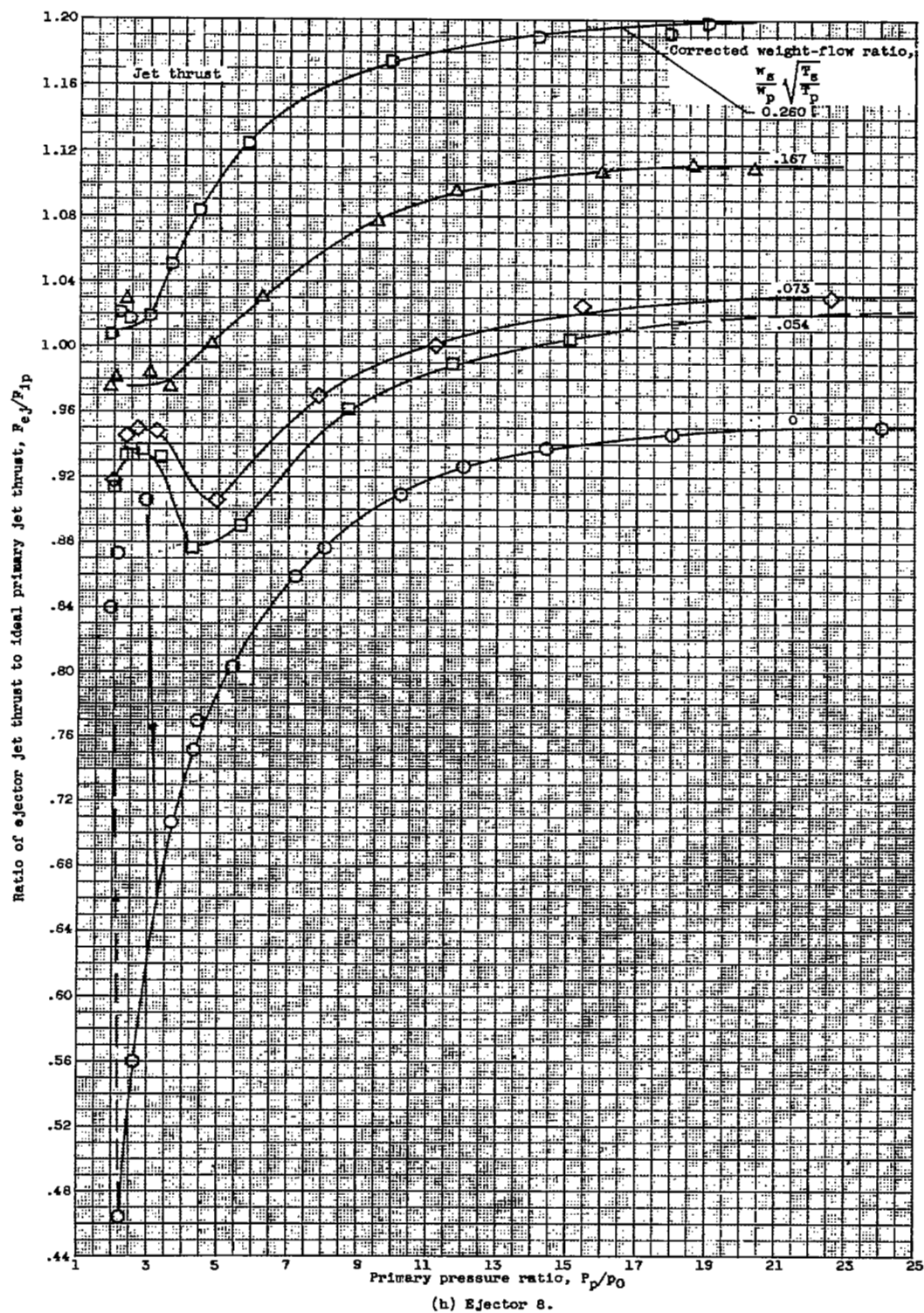Figure 3. - Continued. Performance of divergent-shroud ejectors.
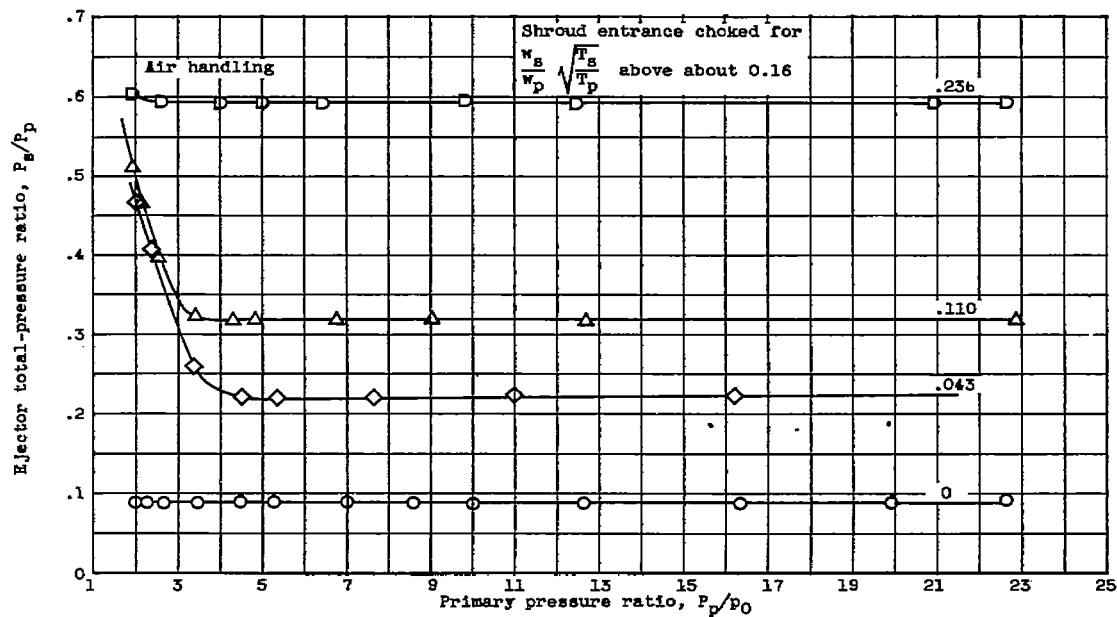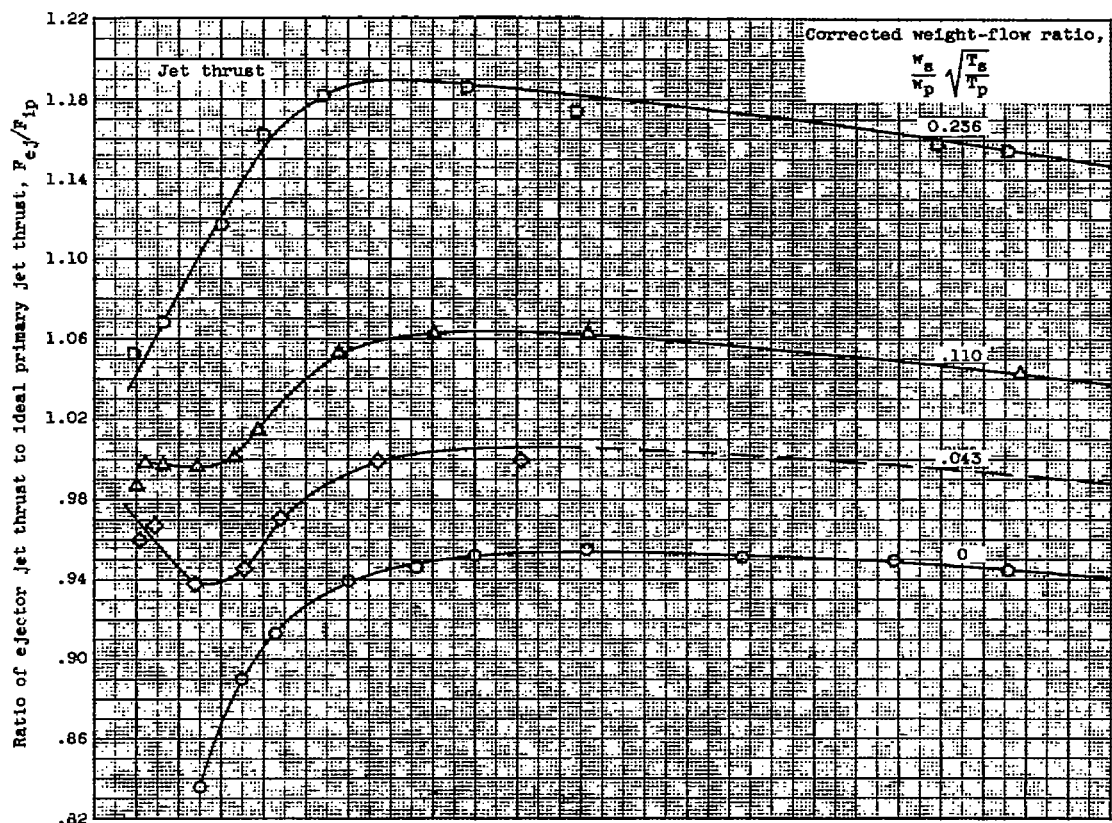
(d) Ejector 4.

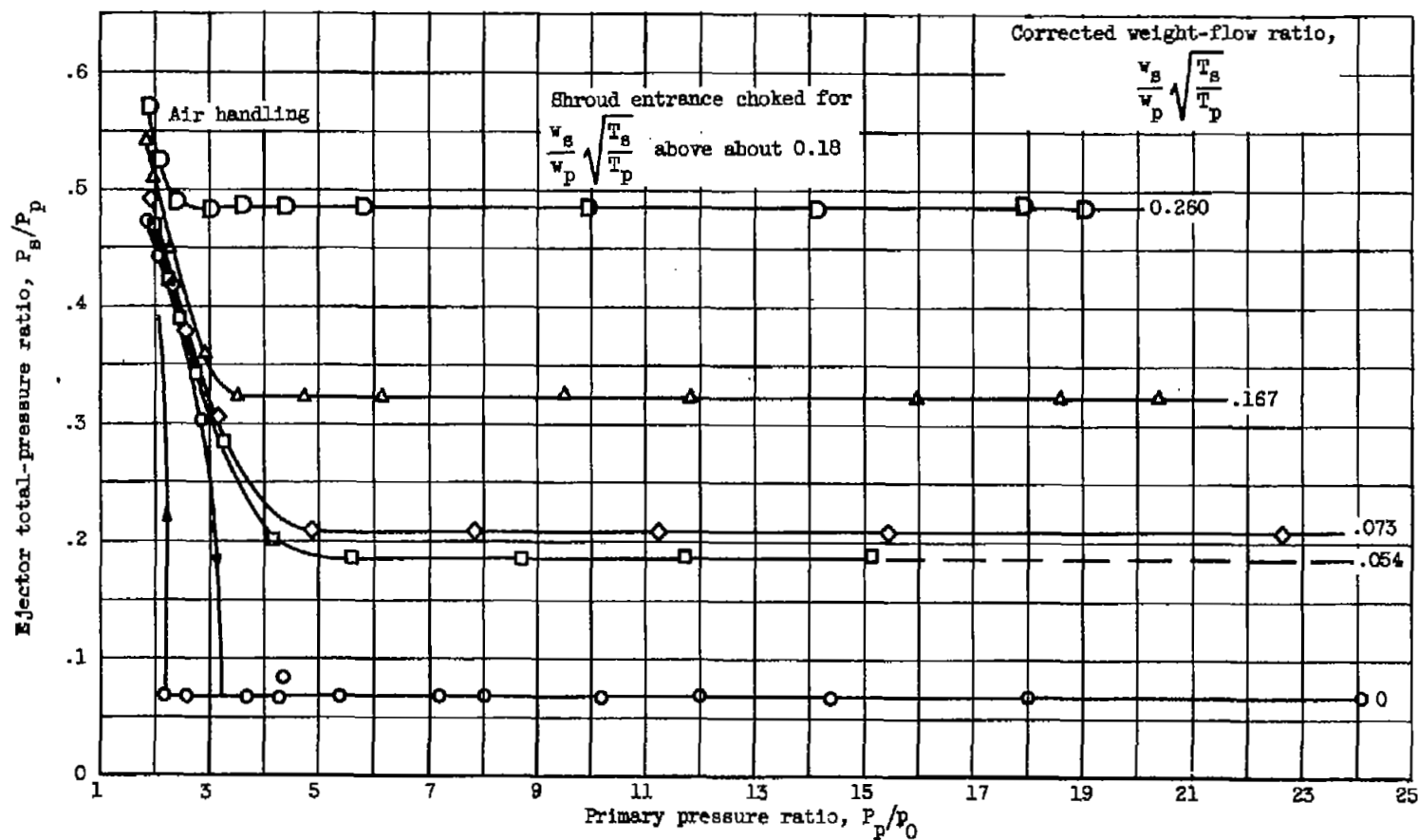Figure 3. – Continued. Performance of divergent-shroud ejectors.

3772
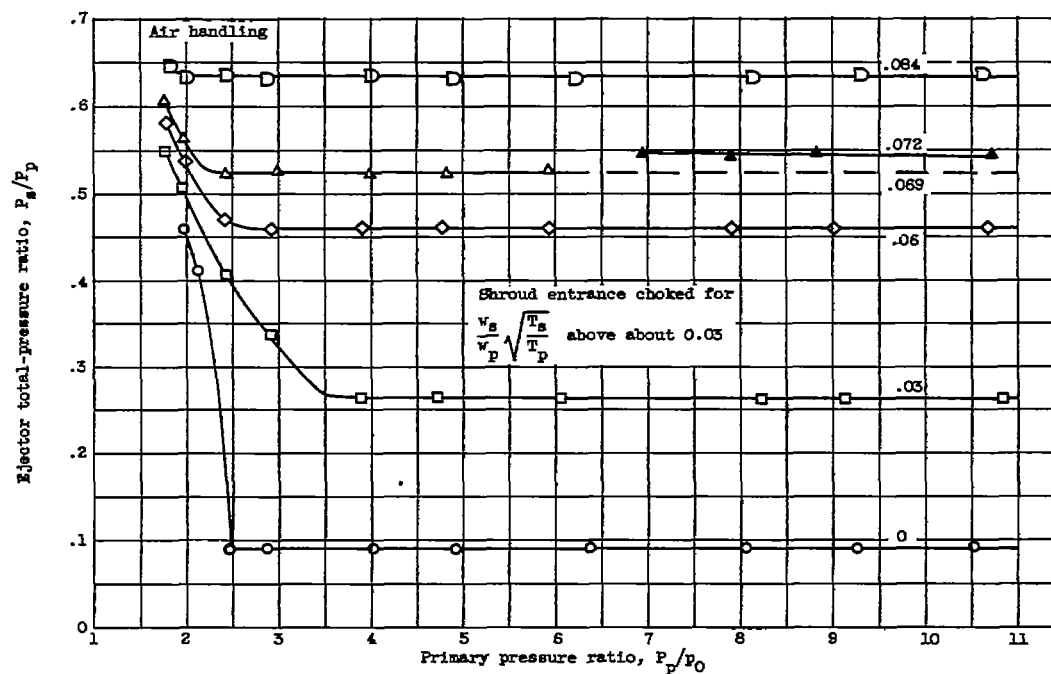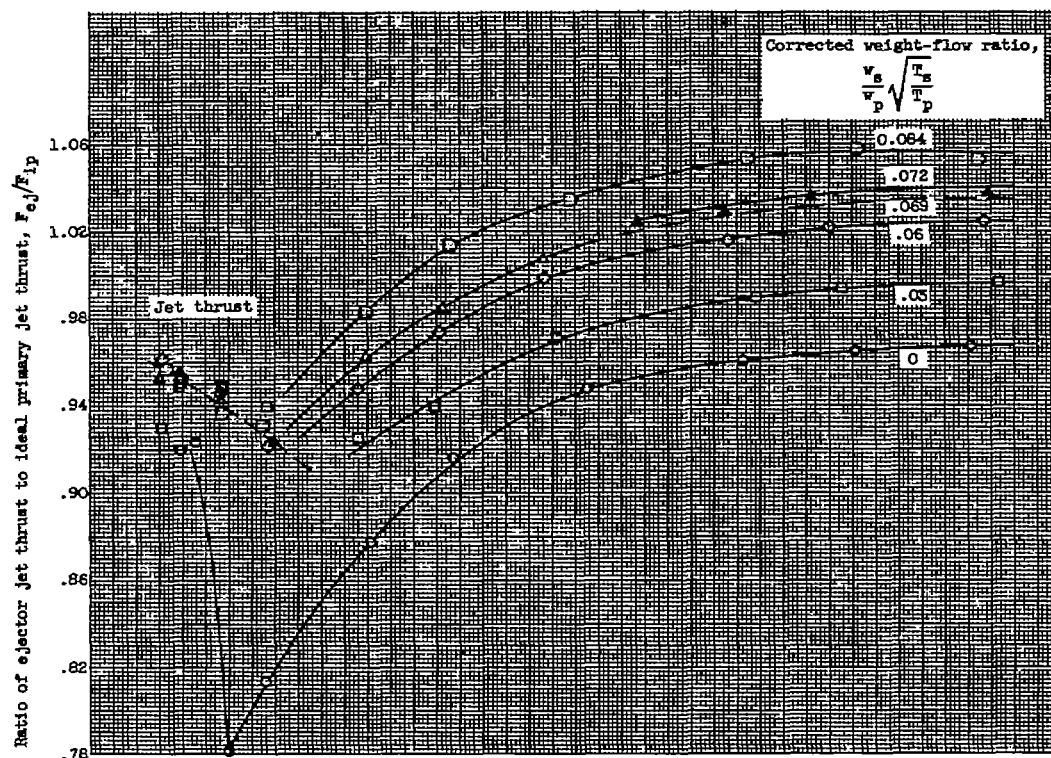
(e) Ejector 5.

Figure 3. - Continued. Performance of divergent-shroud ejectors.
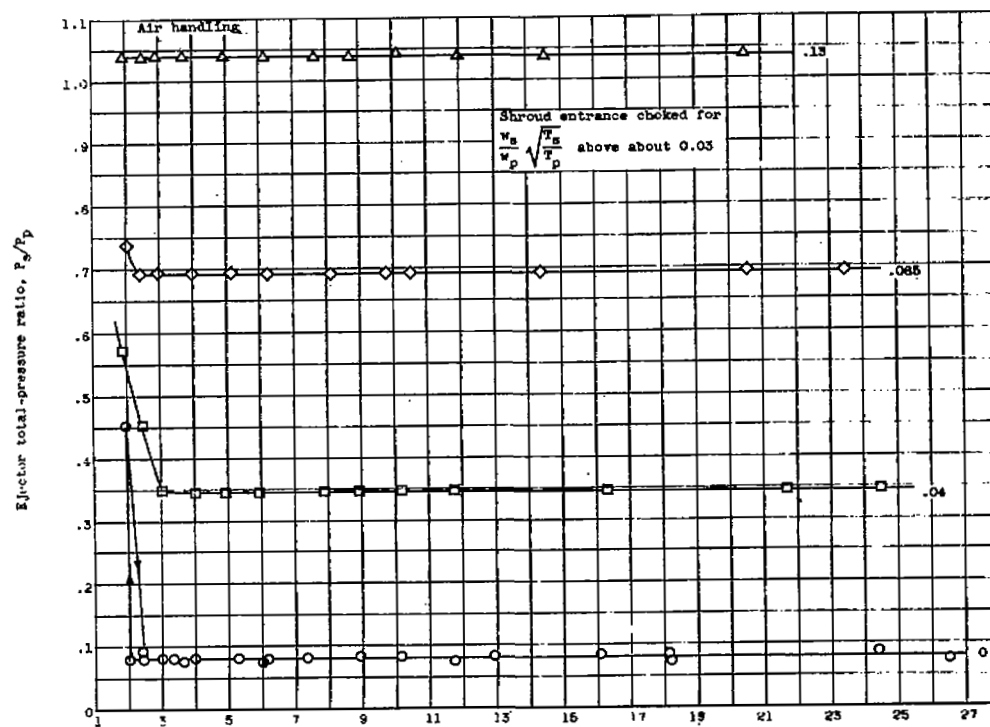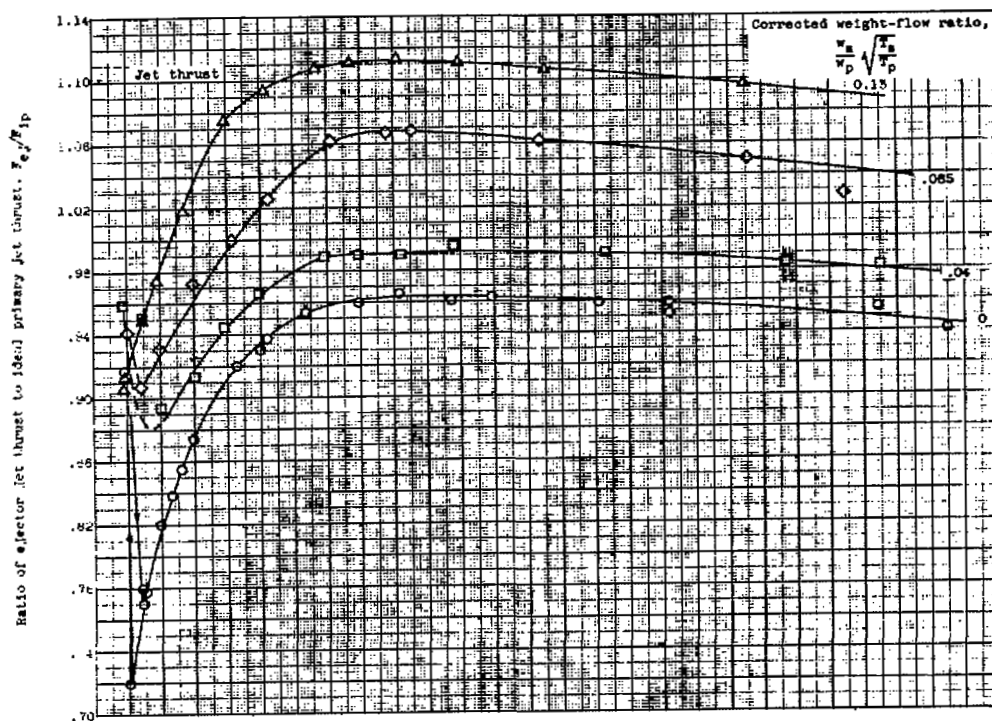
(f) Ejector 6.

Figure 3. - Continued. Performance of divergent-shroud ejectors.

3772

Figure 3. - Continued. Performance of divergent-shroud ejectors.

(g) Concluded. Ejector 7.

Figure 3. - Continued. Performance of divergent-shroud ejectors.

(h) Ejector 8.

Figure 3. - Continued. Performance of divergent-shroud ejectors.

(h) Concluded. Ejector 8.

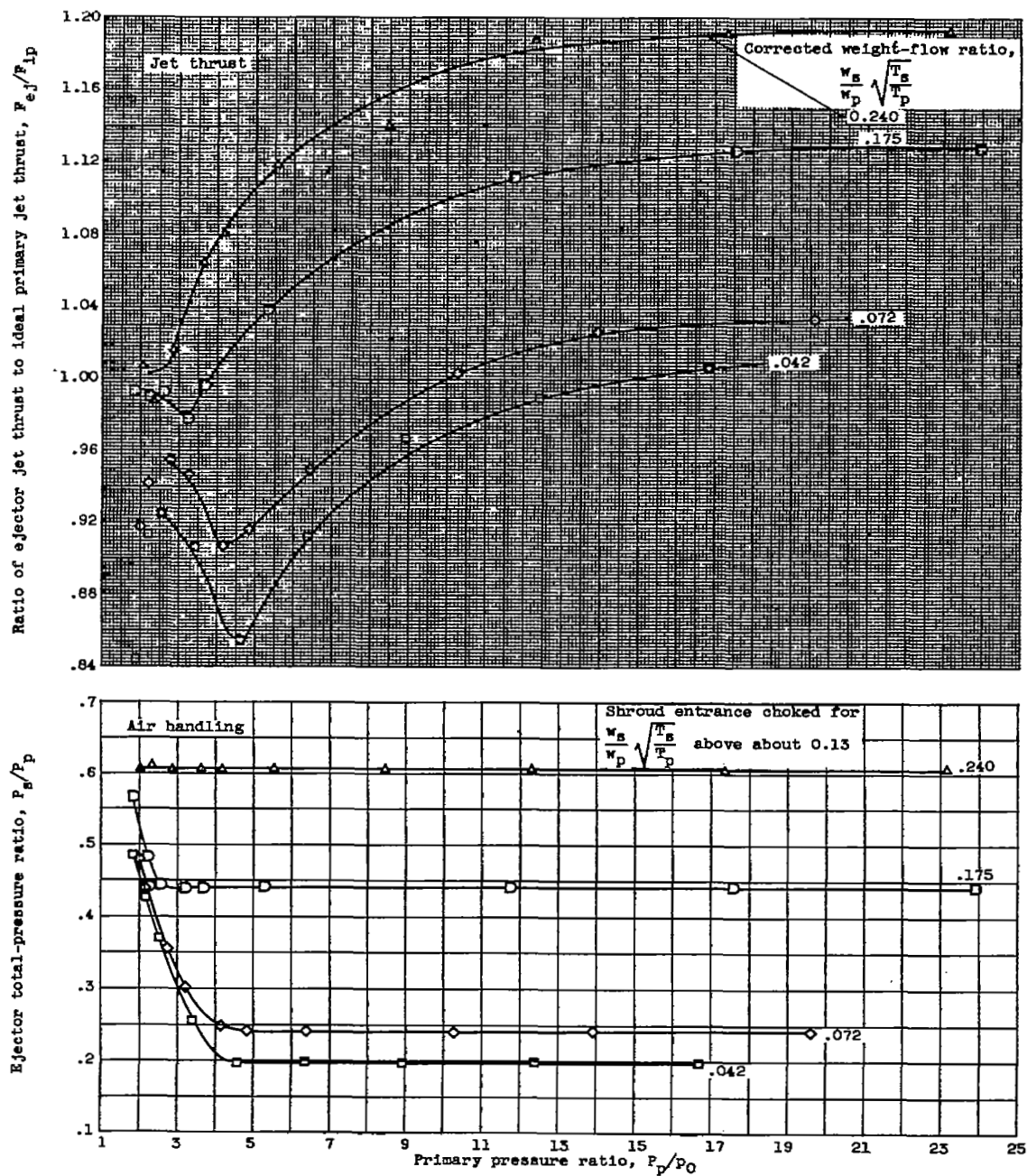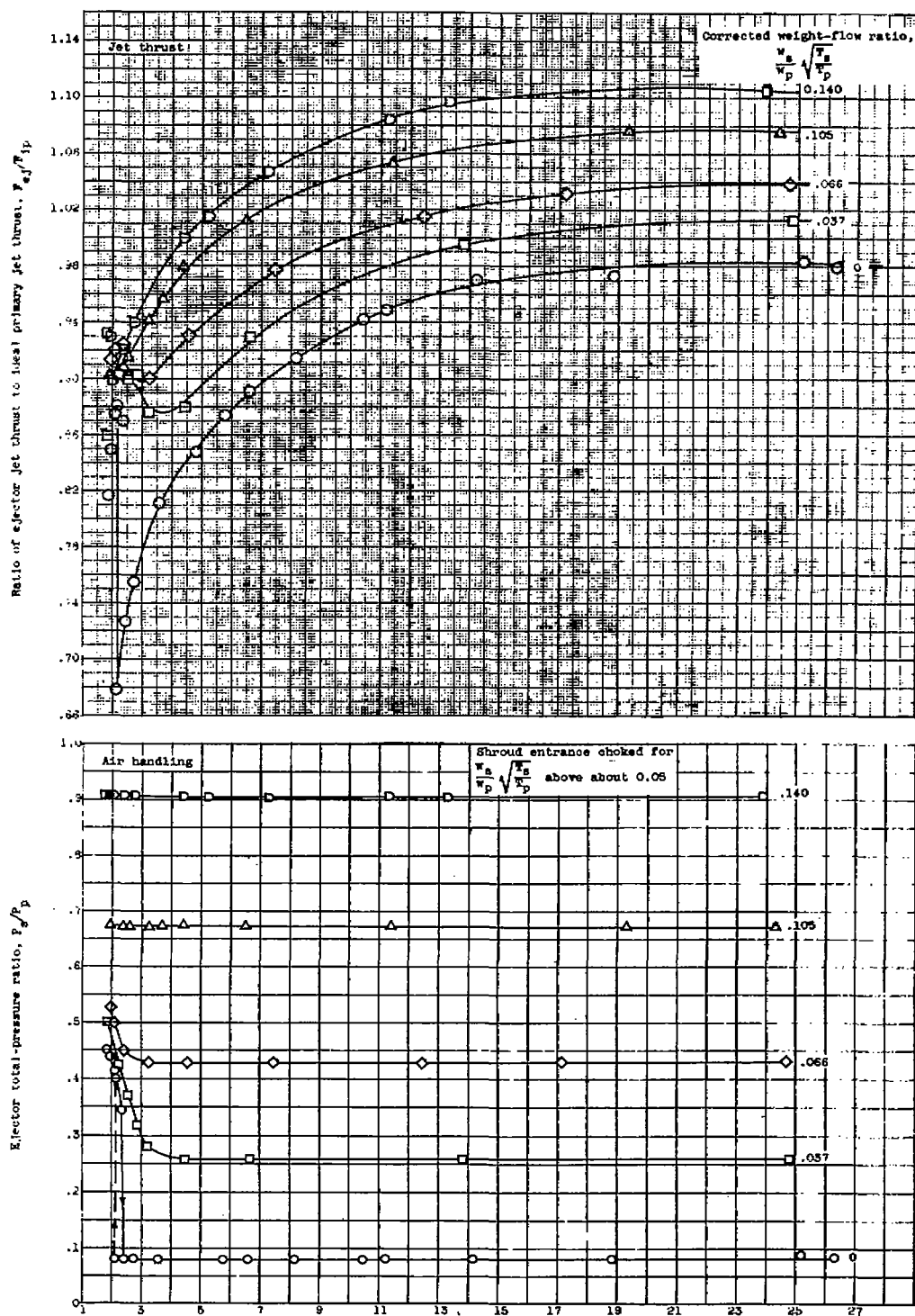Figure 3. - Continued. Performance of divergent-shroud ejectors.

(1) Ejector 9.

Figure 3. - Continued. Performance of divergent-shroud ejectors.

(j) Ejector 10.

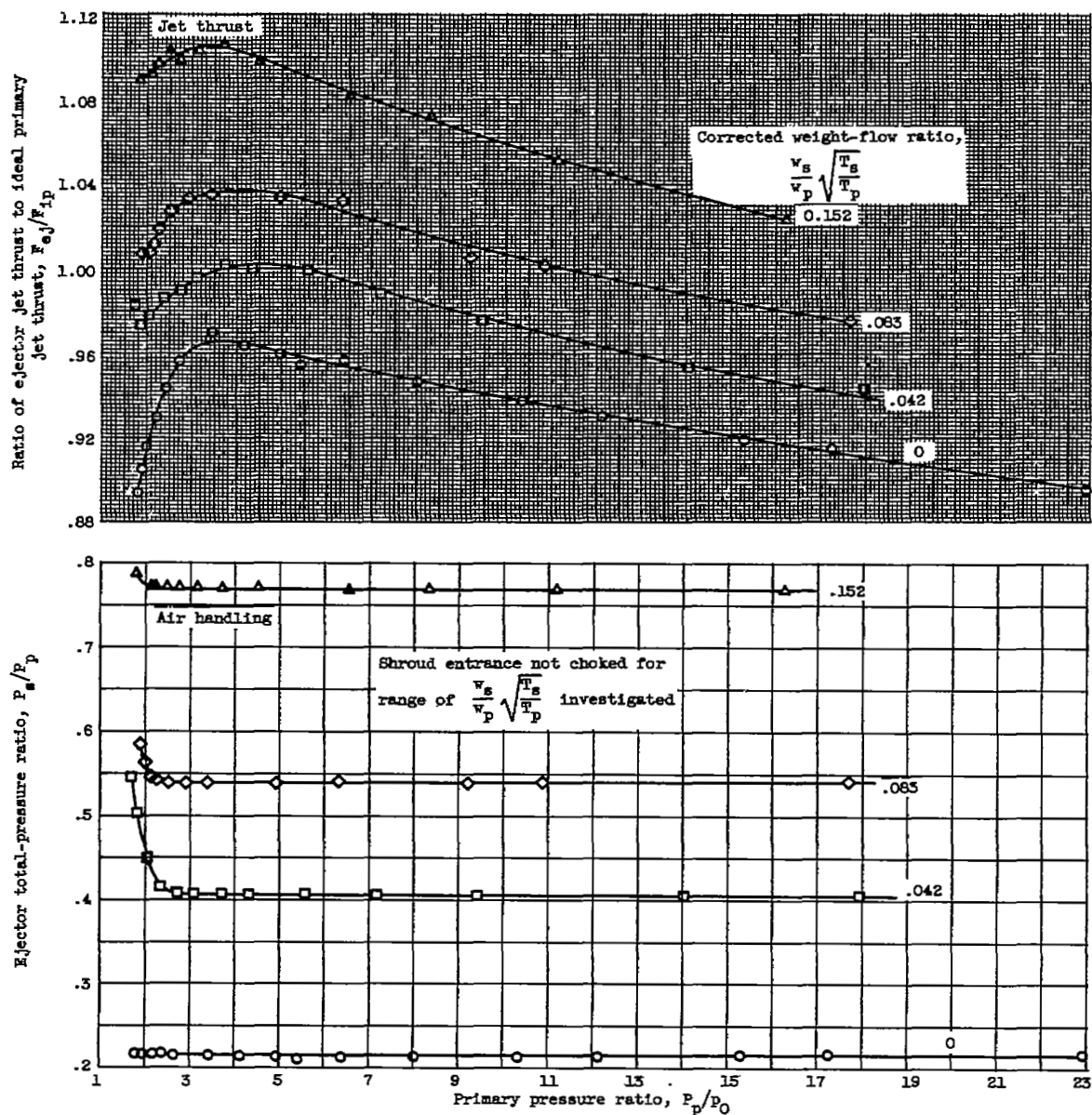Figure 3. - Concluded. Performance of divergent-shroud ejectors.

(a) Ejector 11.

Figure 4. – Performance of cylindrical-shroud ejectors.
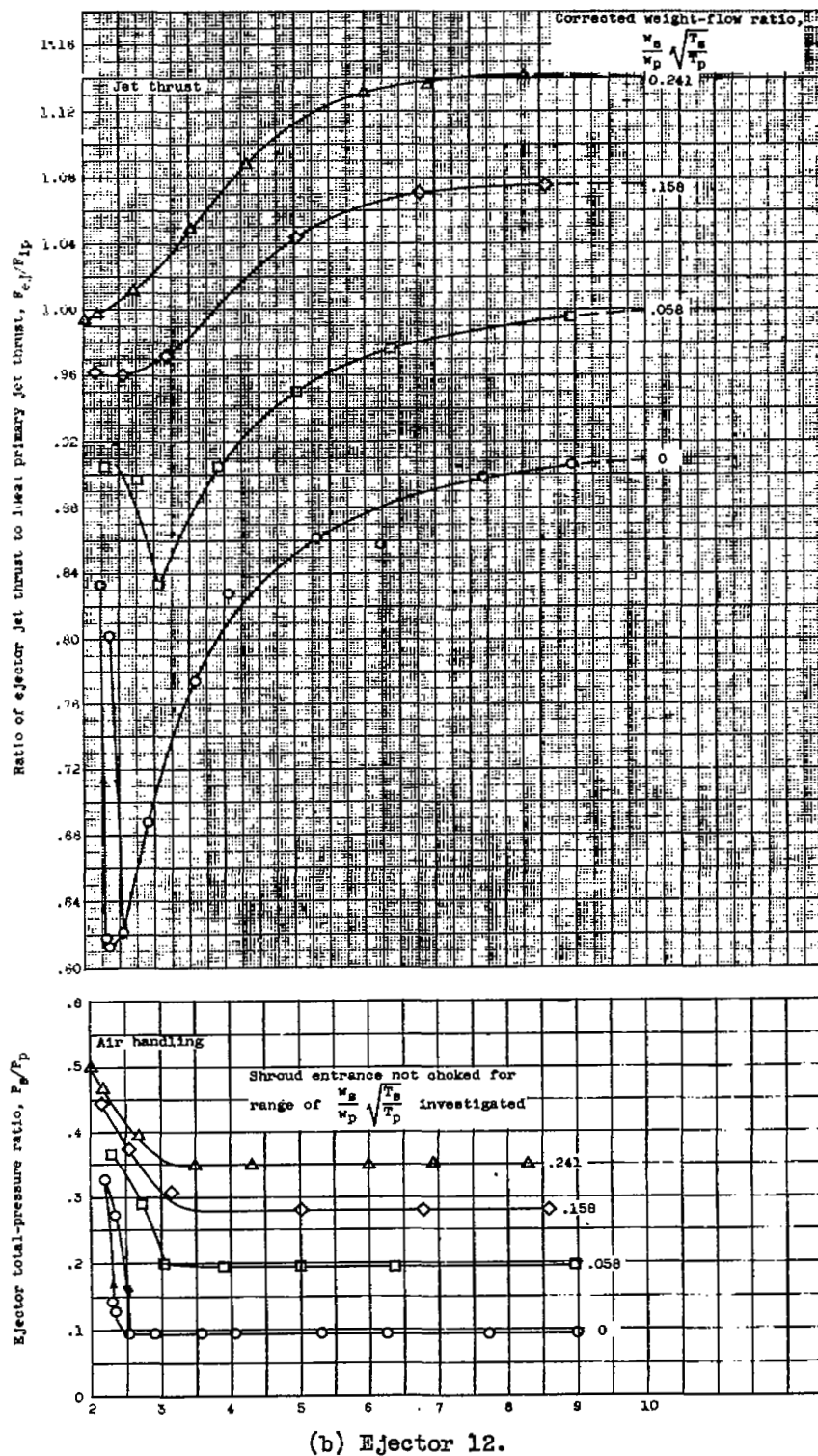
(b) Ejector 12.

Figure 4. - Concluded. Performance of cylindrical-shroud ejectors.
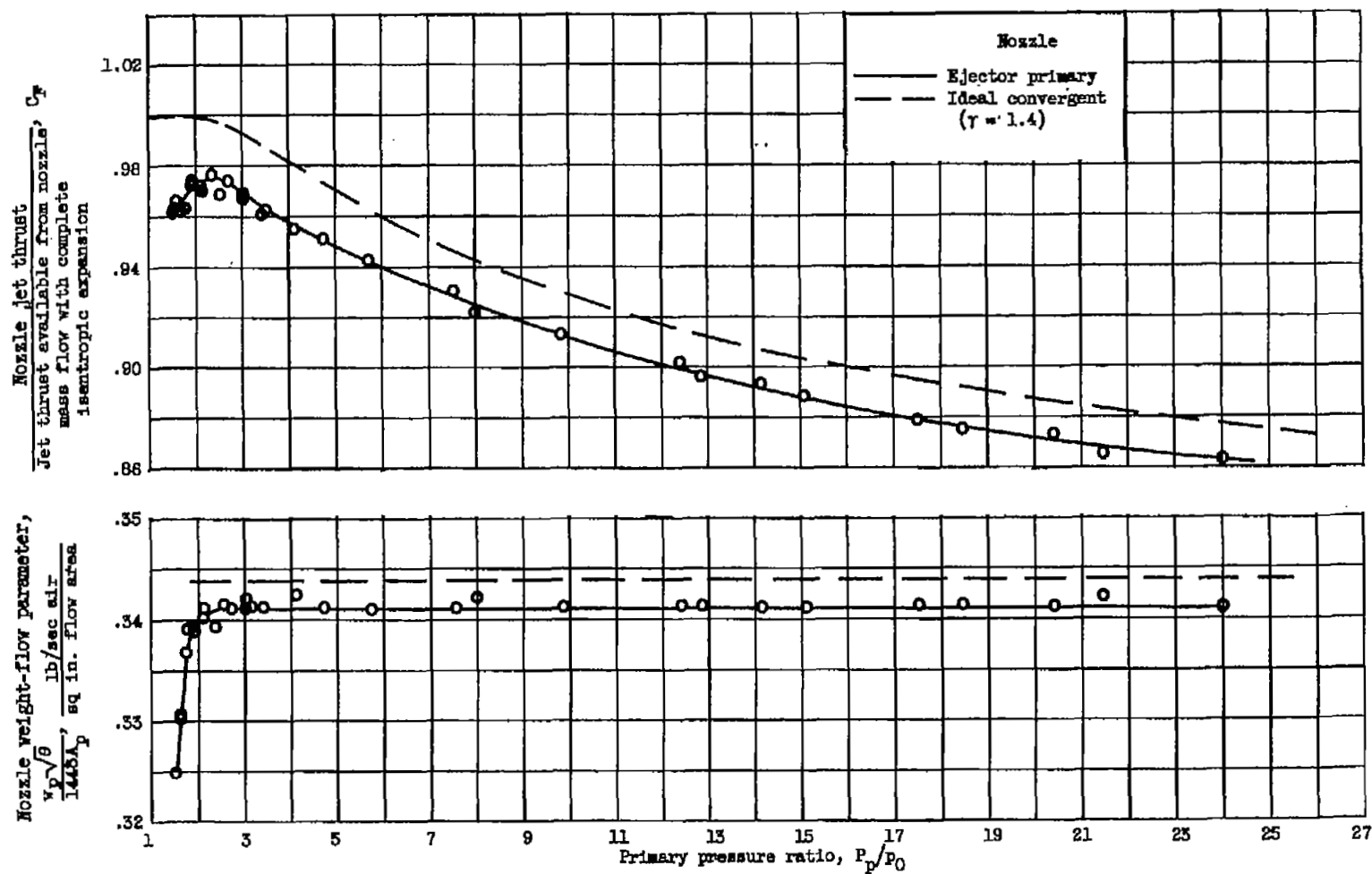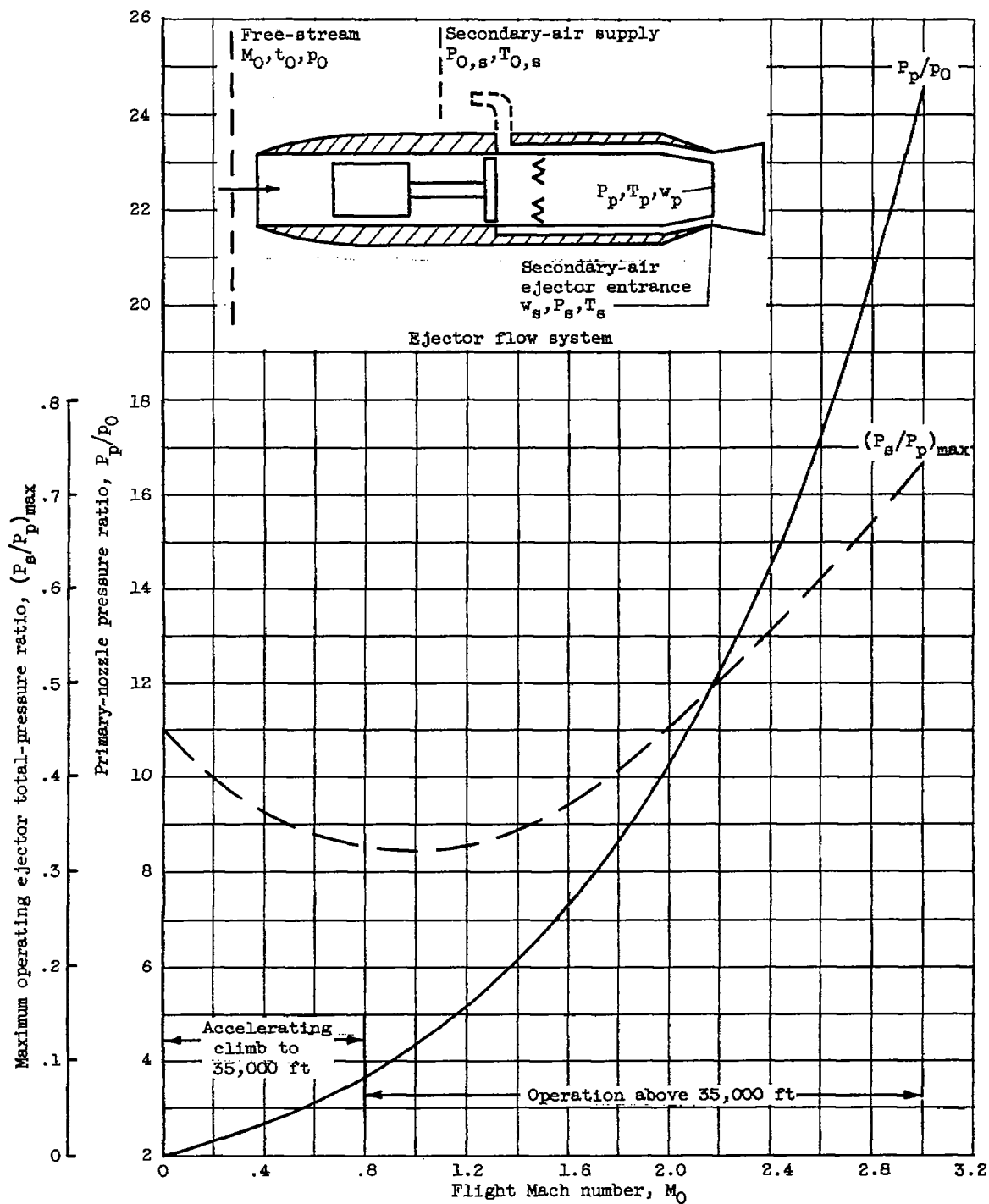
Figure 5. - Primary-nozzle calibration.

Figure 6. - Assumed operating schedule for evaluation of ejector net thrust.
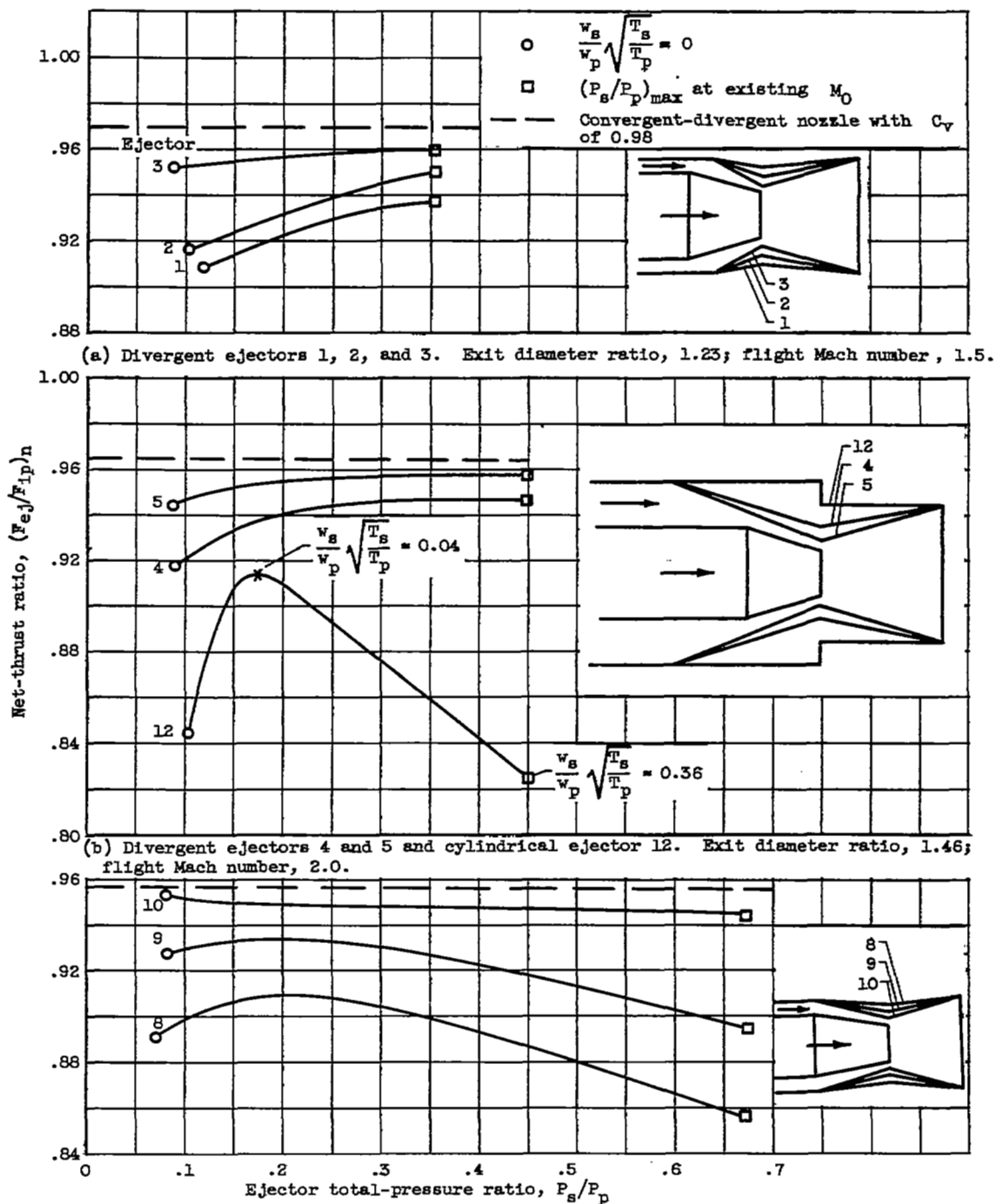
3772

$\frac{w_s}{w_p}\sqrt{\frac{T_s}{T_p}} = 0$

$(P_s/P_p)_{max}$ at existing M_O

Convergent-divergent nozzle with C_V of 0.98

Ejector

3

2

1

3
2
1

(a) Divergent ejectors 1, 2, and 3. Exit diameter ratio, 1.23; flight Mach number, 1.5.

Net-thrust ratio, $(F_{ej}/F_{ip})_n$

12
4
5

5

4

$\frac{w_s}{w_p}\sqrt{\frac{T_s}{T_p}} = 0.04$

12

$\frac{w_s}{w_p}\sqrt{\frac{T_s}{T_p}} = 0.36$

(b) Divergent ejectors 4 and 5 and cylindrical ejector 12. Exit diameter ratio, 1.46; flight Mach number, 2.0.

10

9

8

8
9
10

Ejector total-pressure ratio, P_s/P_p

(c) Divergent ejectors 8, 9, and 10. Exit diameter ratio, 1.82; flight Mach number, 2.8.

Figure 7. - Net-thrust performance of fixed-shroud ejectors at design Mach number. Primary gas temperature, 3500° R.

(a) Divergent-shroud ejectors.

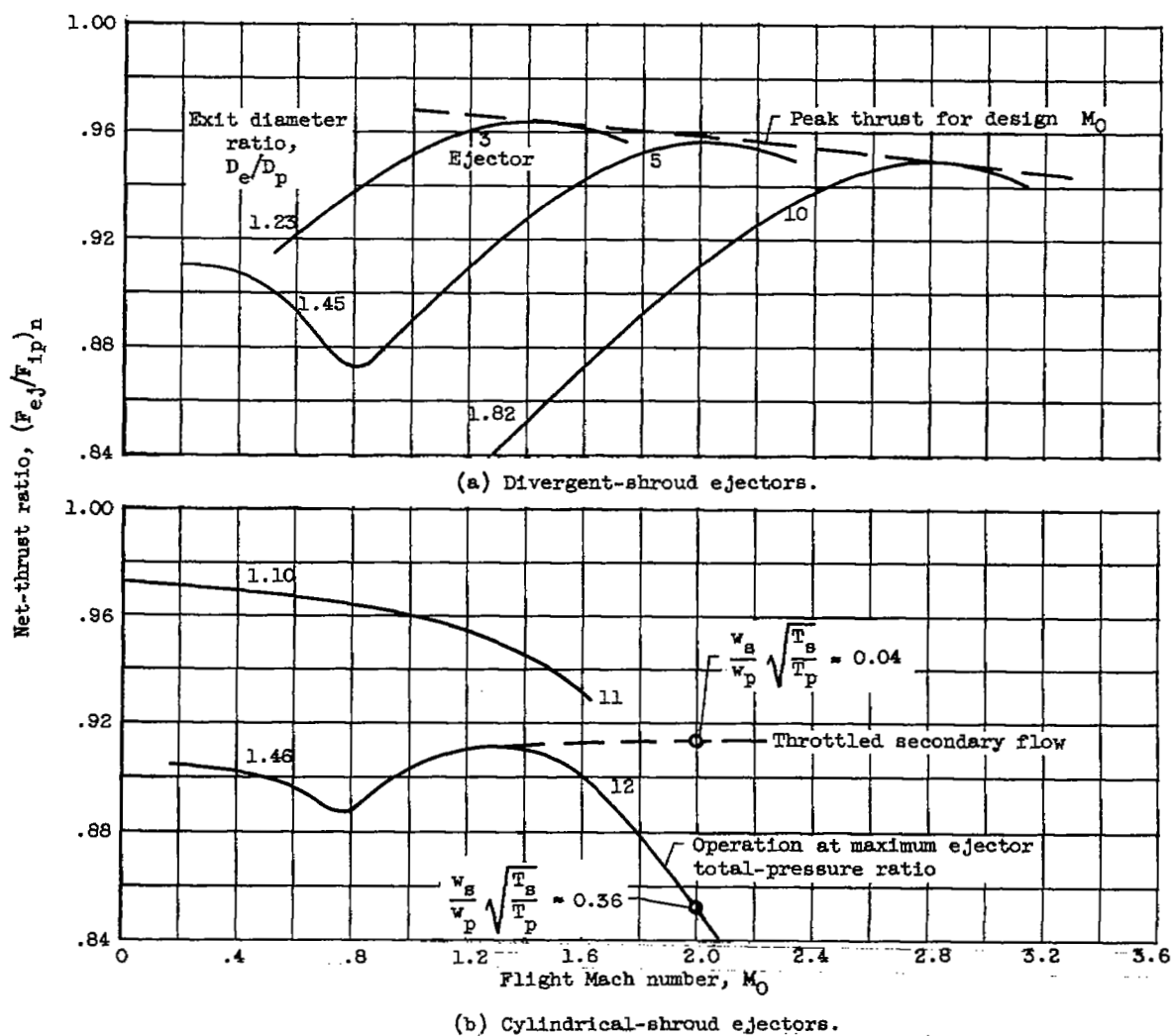(b) Cylindrical-shroud ejectors.

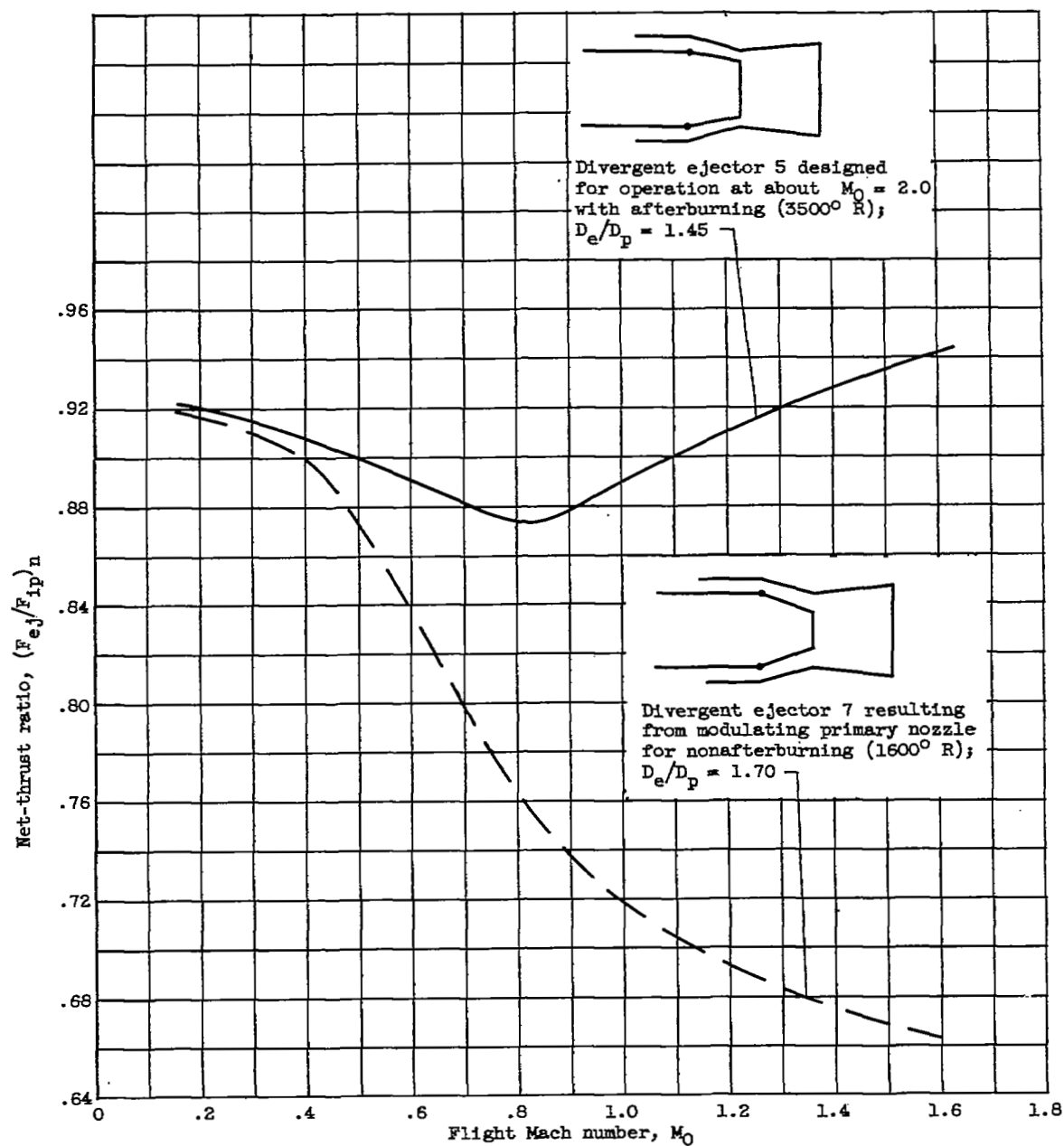Figure 8. - Net-thrust performance of fixed-shroud ejectors over range of flight Mach number. Primary gas temperature, 3500° R.

Figure 9. - Off-design performance of a fixed-shroud divergent ejector.

(a) Fixed primary nozzle. Primary gas temperature, 3500° R.

(b) Fixed primary nozzle. Primary gas temperature, 1600° R.

(c) Variable primary nozzle. Primary gas temperature, 1600° and 3500° R.
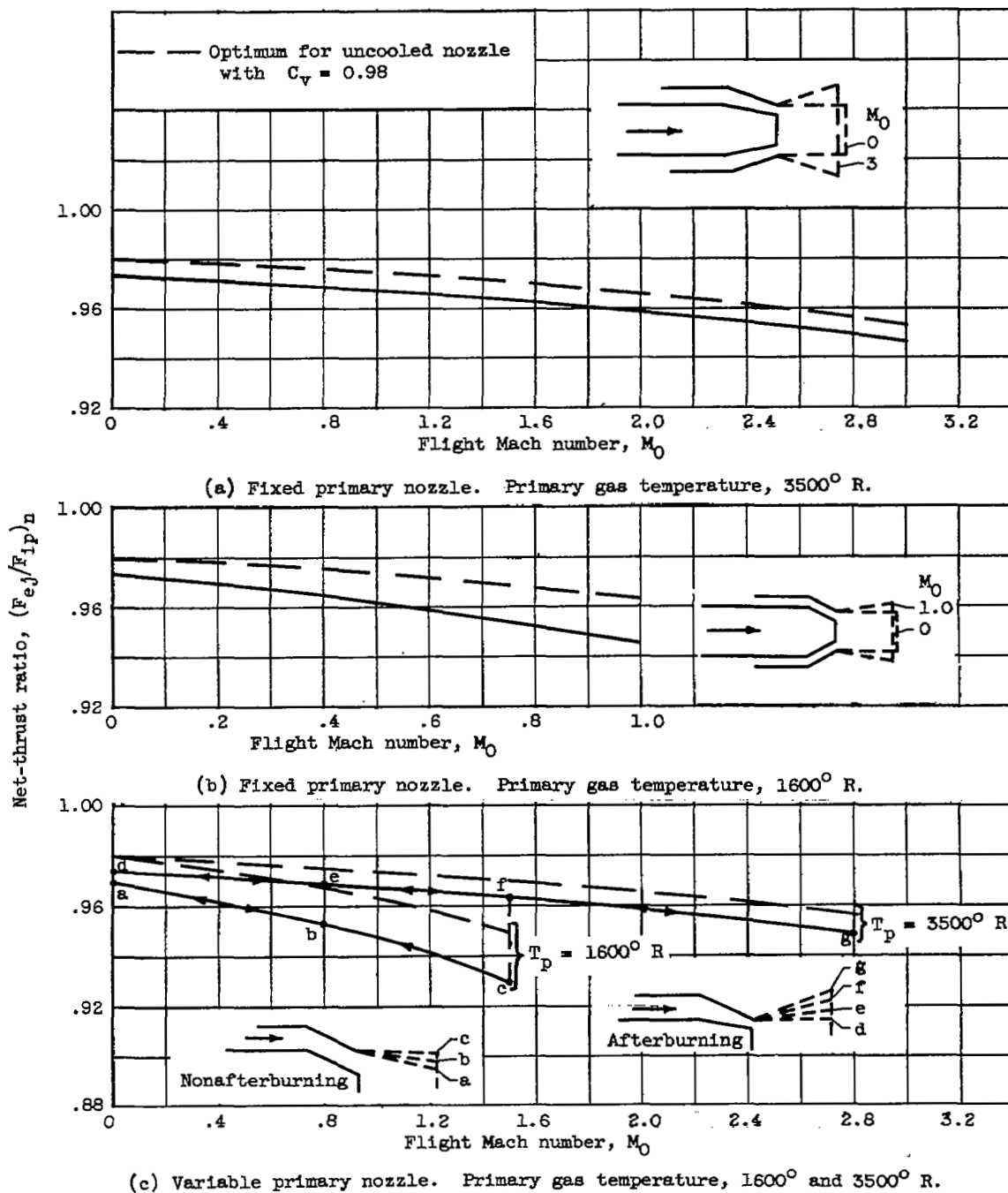
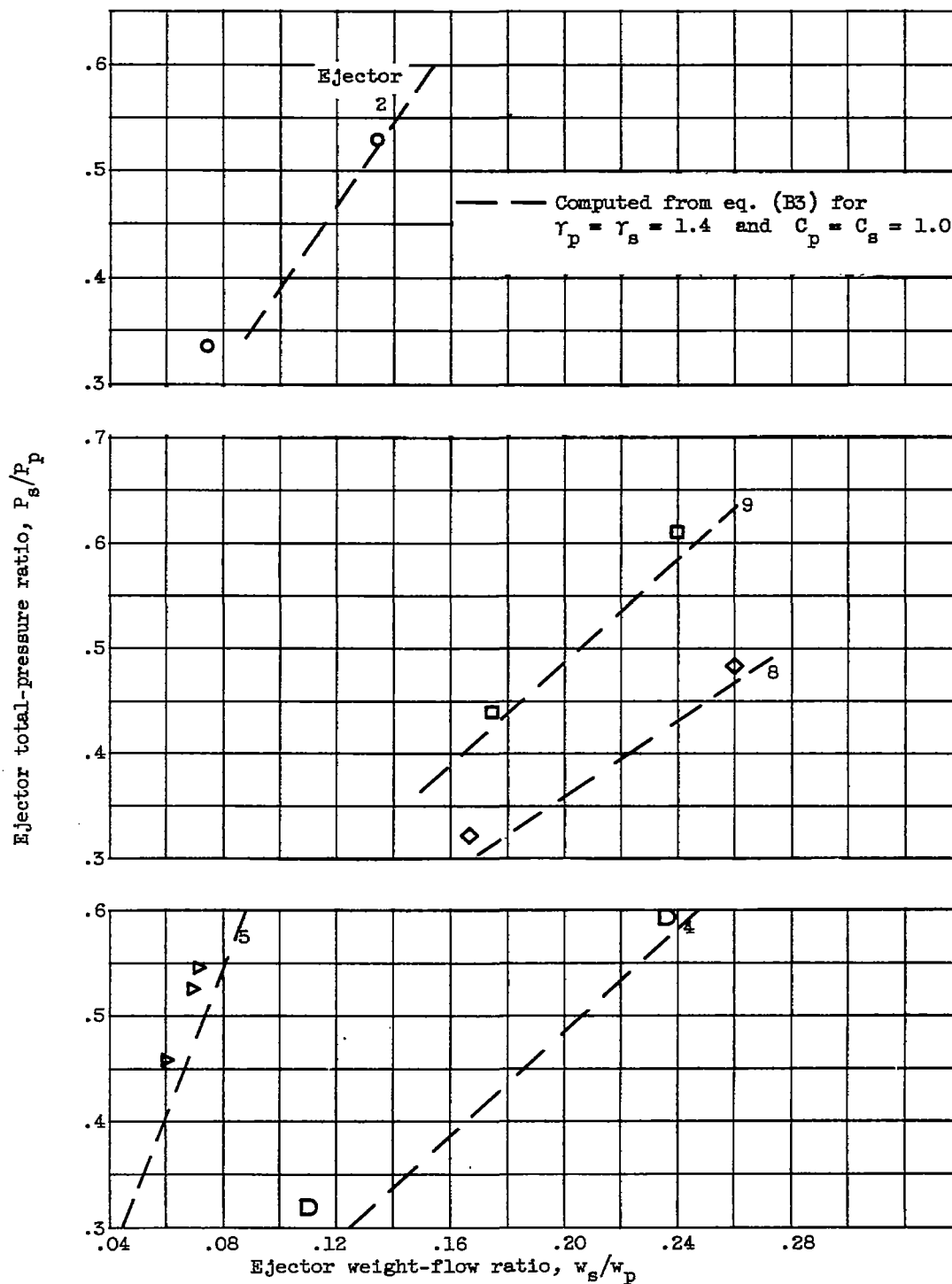Figure 10. - Net-thrust performance of ejectors with variable shroud geometry.

3772

Figure 11. - Comparison of computed and experimental weight-flow ratio
for choked ejectors.

DO NOT REMOVE SLIP FROM MATERIAL

Delete your name from this slip when returning material to the library.

NAME	DATE	MS
Vetter, Jeff	4/27/92	280

NASA Langley (Rev. Dec. 1991)   RIAD N-75